AMERICAN UNIVERSITY OF BEIRUT

MECHANISMS IMPLICATED IN THE ENHANCED SENSITIVITY OF MDA-MB-231 BREAST CANCER CELLS TO ANTI-NEOPLASTIC AGENTS POST SUB-LETHAL HIFU EXPOSURE

by
SARA AHMAD ASSI

A thesis
submitted in partial fulfillment of the requirements
for the degree of Master of Arts
to the Department of Biology
of the Faculty of Arts and Sciences
at the American University of Beirut

Beirut, Lebanon
April, 2016

AMERICAN UNIVERSITY OF BEIRUT

MECHANISMS IMPLICATED IN THE ENHANCED SENSITIVITY OF MDA-MB-231 BREAST CANCER CELLS TO ANTI-NEOPLASTIC AGENTS POST SUB-LETHAL HIFU EXPOSURE

by

SARA AHMAD ASSI

Approved by:

Dr. Diana E. Jaalouk, Assistant Professor Biology	Advisor
Dr. Rabih S. Talhouk, Professor Biology	Member of Committee
Dr. Ghanem Oweis, Associate Professor Mechanical Engineering	Member of Committee
Dr. Rihab Nasr, Associate Professor Anatomy, Cell Biology & Physiology	Member of Committee

Date of thesis/dissertation defense: April 18, 2016

AMERICAN UNIVERSITY OF BEIRUT

THESIS, DISSERTATION, PROJECT RELEASE FORM

Student Name: _____

Last First Middle

◯ Master's Thesis ◯ Master's Project ◯ Doctoral Dissertation

☐ I authorize the American University of Beirut to: (a) reproduce hard or electronic copies of my thesis, dissertation, or project; (b) include such copies in the archives and digital repositories of the University; and (c) make freely available such copies to third parties for research or educational purposes.

☐ I authorize the American University of Beirut, **three years after the date of submitting my thesis, dissertation, or project,** to: (a) reproduce hard or electronic copies of it; (b) include such copies in the archives and digital repositories of the University; and (c) make freely available such copies to third parties for research or educational purposes.

_____

Signature Date

ACKNOWLEDGMENT

There are many people that I would like to thank when looking back to my years at AUB. First and foremost, I am grateful and thankful for my advisor, Dr. Diana Jaalouk, for guiding me and supporting me along the years. I would like to thank you for giving me the opportunity to pursue my MSc thesis in your laboratory and for being patient, understanding, motivating and encouraging during the whole process. Your expertise, immense knowledge and guidance added greatly to my graduate experience. In addition, I am grateful for having taken several courses with you including the advanced cell and molecular biology course, cardiovascular research course and the cancer course. You have set an example of excellence as a researcher, mentor, and professor.

It is also a great pleasure for me to thank my thesis committee members, Dr. Rabih Talhouk, Dr. Ghanem Oweis and Dr. Rihab Nasr for accepting to serve on my committee. Thank you for your continuous support, encouragement, feedback and insightful ideas throughout my MSc study. Dr. Ghanem, Hussein, and Wadih, thank you for all your efforts put on this collaboration. We faced so many hardships and challenges, and thankfully it all worked out eventually. Dr. Rihab, thank you for allowing me to be a member of Amalouna team. It truly means a lot to me.

I would also like to express my sincere gratitude to Dr. Nisreen Alwan who is not only a dear friend to me but has also been providing me with statistical help ever since I joined the MSc Program in the biology department.

I want to thank the amazing DJ lab members Hind Zahr, Dima El Harakeh, Ingrid Younes, Dana Sedki, Ranim Daw and Elvira Dibo. I could not have imagined having a better team to work with. Thank you for all the amazing memories and moments we've shared. You made the difficult and stressful times easier to tolerate. Hind, Dima and Ingrid, thank you for contributing to my training when I first arrived to the laboratory. I truly learnt from the best. Dima, you did not just help me acquire the confocal images but you really were my backbone along the way. I cannot thank you enough.

I am very much grateful to my friend Patrick Aouad who supported me in so many ways and was always there to help me along the way. I would also like to thank Tamara Abu Matar for helping me with the FlowJo program. I am also grateful for all the amazing friends I've made at the department. Each one of you made this journey unforgettable.

Finally, I would especially like to thank my amazing family for the love, support, and constant encouragement I have gotten during my MSc study. You are the chocolate of the earth, and I could not have done this without you.

AN ABSTRACT OF THE THESIS OF

Sara Ahmad Assi for Master of Science
Major: Biology

Title: Mechanisms implicated in the enhanced sensitivity of MDA-MB-231 breast cancer cells to anti-neoplastic agents post sub-lethal HIFU exposure

High Intensity Focused Ultrasound (HIFU) is an ex-corporeal medical device that was first introduced in the 1940s for the treatment of neurological disorders and has been subjected to several improvements since then. It is a non-invasive and non-ionizing therapeutic method that is now utilized to destroy a wide variety of tumors including breast cancer. At the focal point where the acoustic waves are intensified, cell death can result from cavitation and/or thermal ablation effects. However, the effects of sub-lethal HIFU exposure on cell function are not clearly understood. Previous work from our laboratory showed that sub-lethal HIFU exposure of MDA-MB-231 breast cancer cells *in vitro* results in significant alterations in transcript expression of a number of mechanosensitive genes, including *Cav-1* gene which encodes for caveolin-1 protein. Moreover, there was enhanced cellular sensitivity to suboptimal cytotoxic doses of Paclitaxel and Doxil. Therefore, we hypothesized that sonoporation and/or caveolin-dependent endocytosis are among the mechanisms involved in this enhanced *in vitro* sensitivity of MDA-MB-231 cells post sub-lethal HIFU. For the purpose of this study, we utilized a commercial HIFU setup that operates at the fundamental resonance of 0.5MHz. To examine if sonoporation is implicated in the enhanced drug uptake post sub-lethal HIFU, we assessed the uptake of FITC-dextran by two methods: cell fixation followed by flow cytometry or laser confocal microscopic imaging and analysis. To determine if caveolin-dependent endocytosis is implicated as a mechanism of enhanced drug uptake, we pre-treated the cells with Genistein, a specific potent inhibitor of this pathway. Cellular viability was quantified using trypan blue vital stain exclusion assay. We found no significant change in FITC-dextran uptake in MDA-MB-231 cells post sub-lethal HIFU exposure at 30hr prior to the *in vitro* addition of agents by flow cytometry and laser confocal microscopy. Similarly, no significant change in FITC-dextran uptake was observed at the 6hr time point by laser confocal microscopy. Interestingly, pre-treatment with Genistein resulted in a significant increase in cellular viability in comparison to control group particularly 30hr prior to the *in vitro* addition of Doxil. Taken together, our findings highlight the implication of caveolae-dependent endocytosis in cellular sensitivity of MDA-MB-231 breast cancer cells to suboptimal cytotoxic doses of agents post sub-lethal HIFU exposure. Ongoing work and future directions will focus on validating the latter results using various levels of exposure.

CONTENTS

ILLUSTRATIONS

ABBREVIATIONS

%	Percent
/	Per
µM	Micro Molar
µg	Micro Gram
µl	Micro Liter
ABCB	ATP-binding cassette sub-family B
Bcl-2	B-cell lymphoma 2
BRCA	Breast Cancer Susceptibility gene
Cav-1	Caveolin-1
Cav-2	Caveolin-2
Cav-3	Caveolin-3
CDK	Cyclin dependent kinase
CK5/6	Cytokeratin 5/6
DAPI	4', 6-Diamidino-2-Phenylindole
DCIS	Ductal Carcinoma in situ
ddH_2O	Double distilled water
DMSO	Dimethyl sufoxide
DNA	Deoxyribonucleic Acid
DNMT1	DNA Methyl Transferase 1
ECM	Extracellular Matrix

EGF	Epithelial Growth Factor
EGFR	Epidermal Growth Factor Receptor
ER	Endoplasmic reticulum
ER	Estrogen receptor
et al.	et allii (and others)
FBS	Fetal Bovine Serum
FDA	Food and drug administration
FGF	Fibroblast Growth Factor
FITC	Fluorescein isothiocyanate
g	grams
HER	Human Epidermal Growth Factor Receptor
HGF	Hepatoctye Growth Factor
HIFU	High Intensity Focused Ultrasound
HR	Hormone Receptor
hr	Hour
Hz	Hertz
IBC	Invasive Lobular Carcinoma
IDC	Invasive Ductal Carcinoma
IGF1	Insulin-epidermal Growth Factor
In Situ	On Site
KDa	Kilo Dalton
LCIS	Lobular Carcinoma in situ
MAPK	Mitogen Activated Protein Kinase
MCF-10A	Michigan Cancer Foundation cells number 10 A

MCF-7	Michigan Cancer Foundation cells number 7
MDA-MB-231	Monroe Dunaway Anderson Metastatic Breast cancer cells number 231
MDR1	Multi-drug resistance
mg	Milligram
MHC	Major Histocompatibility Complex
min	Minute
miR	Micro RNA (mRNA)
ml	Milliliter
mm	Millimeters
MMP	Matrix Metalloproteinase
MRI	Magnetic Resonance Imaging
msec	Millisecond
NES1	Normal Epithelial cell-specific 1
nM	Nano Molar
^{o}C	Degrees Celsius
P	p-value
P53	Tumor Protein 53
PBS	Phosphate Buffered Saline
PCR	Polymerase Chain Reaction
PDGF	Platelet Derived Growth Factor
PFA	Paraformaldehyde
PI3K	Phosphoinositide 3 kinase
PR	Progesterone Receptor
RNA	RiboNucleic Acid

RPMI	Rose Park Memorial Institute
Sec	Second
SEM	Standard Error of the Mean
siRNA	Short interfering Ribonucleic acid
Src	Proto-oncogene Tyrosine-protein Kinase
SV40	Simian Virus 40
SYK	Spleen Tyrosine Kinase
TGF- β	Transforming Growth Factor-β
VEGF	Vascular Endothelial Growth Factor
Vpp	Peak to Peak Voltage
WNT	Wingless-type MMTV (mouse mammary tumor virus)

CHAPTER I

INTRODUCTION

A. General Overview

High Intensity Focused Ultrasound (HIFU) is a therapeutic modality used to destroy solid tumors. At the focal point, cell death can result from cavitation and/or thermal ablation effects. However, the effects of sub-lethal HIFU exposure on cell function are not well understood. Scientists have reported that pressure/tension waves post HIFU exposure cause cellular deformations at the tissue level. Subsequently, previous colleagues from our laboratory were interested to see if there is any alteration in the expression of a selection of mechanosensitive genes post sub-lethal HIFU exposure. Previous work from our laboratory showed that sub-lethal HIFU exposure (i.e., exposure where cells are receiving residual HIFU) of MDA-MB-231 breast cancer cells *in vitro* results in significant alterations in transcript expression of a number of mechanosensitive genes, including *Cav-1* gene (α-isoform) which encodes for caveolin-1 protein. During that time, a study published in 2012 showed that the *Cav-1* gene (α-isoform) facilitates apoptosis in cancer cells in response to the drug Paclitaxel (Shajahan et al., 2012). Subsequently, we were interested to see if there was enhanced cellular sensitivity to suboptimal cytotoxic doses of Paclitaxel and Doxorubicin post sub-lethal HIFU exposure and indeed enhanced cytotoxic response was obtained to anti-neoplastic agents post sub-lethal HIFU exposure. What we were next interested in is to decipher the mechanisms that are implicated in this enhanced in vitro sensitivity. Therefore, we rationalized that sonoporation and/or caveolae-dependent

endocytosis are among the mechanisms involved in this enhanced *in vitro* sensitivity of MDA-MB-231 cells post sub-lethal HIFU.

B. Mammary Gland

1. Overview

The mammary gland is a secretary organ located in the breasts of female mammals and is distinguished by its ability to produce milk in order to feed and nurture young offspring. It is composed of multiple cell types, including epithelial cells that are comprised of apically oriented luminal cells lining the milk ducts and alveoli and of basally oriented myoepithelial cells in contact with the basement membrane; adipocytes that constitute a large fraction of the stromal fat pad; fibroblasts, immune, lymphatic and vascular cells that are present throughout the fat pad (Inman et al., 2015).

2. Development Processes & Pathways

The development of a mammary gland begins during embryonic life, pauses at birth and carries on at puberty through adulthood (Watson & Khaled, 2008). What is mainly known about this development is derived from mouse models which should be projected to humans, while bearing in mind the physical and genetic variability between both species (Lanigan et al., 2007). In mice, mammary gland development is first observed on day 10 of gestation with the emergence of mammary lines between the fore and hind limb buds. Within 24-36 hours of the formation of the mammary lines, five pairs of lens-

shaped mammary placodes are observed. At embryonic day 14, each mammary placode develops and invaginates into the underlying mesenchyme to form a mammary bud. This is followed by ductal branching which occurs around week 16 and continuous until puberty. Simultaneously, the ductal lumen along with the nipples begins to develop. This development will continue throughout puberty reaching pregnancy, where the maturation of the milk producing glands will be achieved (Cowin & Wysolmerski, 2010). Development of the mammary gland involves a series of integrated signaling specifically during puberty. Paracrine signaling is set in motion by ovarian and pituitary hormones, including estrogen and growth hormones through the release of various endocrine signals, such as IGF1, HGF, EGF and FGF while autocrine signaling is triggered by cues such as transforming growth factor-β (TGF-β) that negatively controls mammary gland morphogenesis by inducing ECM production or by activating non-canonical WNT signaling to inhibit proliferation and possibly to regulate cell adhesion and migration (Gjorevski et al., 2011).

C. Breast Cancer

1. Overview

Breast cancer is not only the most frequent type of cancer found in women but it is also considered to be the second leading cause of death among women worldwide (Youlden et al., 2014). Many factors are known to increase the risk of breast cancer such as obesity, age, hormonal supplements, lack of breastfeeding, and family history. Types of breast cancer vary according to the tissue and organs they originate from. The most common types of breast cancer begins in cells of the ducts where abnormal cells replace

normal epithelial cells of the breast and this is referred to as ductal carcinoma in situ (DCIS). When it breaks through the wall of the ducts and spreads from where it has begun to surrounding tissue, it is referred to as invasive ductal carcinoma (IDC). Breast cancer may also begin in the cells of the lobules where it is referred to as lobular carcinoma in situ (LCIS). Likewise, when it spreads and becomes infiltrating, it is referred to as invasive lobular carcinoma (IBC) (American Cancer Society, 2015).

2. Molecular Subtypes of Breast Cancer

Breast cancer is a heterogeneous group of diseases that is distinguished by at least four main molecular subtypes identified based on the traditional biological marker profiling including the presence or absence of hormone (estrogen or progesterone) receptors (HR+/HR-) and excess levels of human epidermal growth factor receptor 2 (HER2+/HER2-). The four main molecular subtypes are luminal A (HR+/HER2-) which expresses either of the hormone receptors or both but not HER2 receptor; luminal B which also expresses any or both of the hormone receptors but are further defined by the expression of HER2 or Ki67 which is an indicator of a great amount of actively dividing cells; triple negative (HR-/HER2-) which do not express any hormone receptors nor the HER2 receptor; and HER2 enriched (HR-/HER2+) which do not express any of the hormone receptors as well but produces excess of HER2 receptor. It is worth mentioning that classification methods are being refined as various molecular techniques including gene expression profiling techniques evolve (American Cancer Society, 2015). Moreover, each of the molecular subtypes is associated with a distinct course of treatment and

prognosis. In order to generate the most effective treatment, a wide variety of cell lines have been established *in vitro* to represent the heterogeneity of breast cancers. Among the various breast cancer cell lines established, MCF-7 falls into the luminal A subtype, BT-474 falls into the luminal B subtype, MDA-MB-231 falls into the triple negative subtype and MDA-MB-453 falls into the HER2 enriched subtype. Noteworthy, many studies have reported that MDA-MB-231 is considered of a basal subtype as well since it expresses the epidermal growth factor receptor (EGFR) in addition to the triple negative phenotype (Subik et al., 2010). One of the defining characteristics of basal like cancers is the expression of CK5/6 and/or EGFR in combination with the lack of expression of ER, PR, and HER2. Some studies have used the terms triple-negative and basal-like interchangeably while others indicated that although there are various similarities between both breast cancers, these two terms are not synonymous (Badve et al., 2011).

3. Pathways Implicated in Breast Cancer

a. Proteins and Mutations Involved

Molecular and genetic events underlying breast cancer development vary greatly among different tumors. Initiation of breast cancer is contributed by mutations of tumor suppressor genes such as p53, BRCA1 and BRCA2 or epigenetic functional inactivation of further tumor suppressor genes such as SYK and NES1 besides to changes in proto-oncogenes, such as HER2/neu (Buchholz et al., 2002). Other mechanisms and pathways that influence tumor development include HER family members which regulate biological processes such as cell survival and differentiation; members of the mitogen activated

protein kinase (MAPK) family that control cell proliferation, differentiation, and survival; phosphatidylinositol 3-kinase (PI3K) pathway that plays a central role in cell growth, cell motility, cell survival, and angiogenesis; and apoptotic signaling pathways. In addition, deregulation of apoptosis plays a key role in tumorigenesis as it allows cancer cells to escape death and therefore become resistant to anticancer treatments. Moreover, angiogenesis is considered a fundamental step in the development of tumors and metastasis so any alteration in angiogenic proteins such as Vascular Endothelial Growth Factor (VEGF) and Platelet Derived Growth Factor (PDGF) serve to play a role in breast cancer development. These proteins are involved in numerous cellular activities including survival, mitogenesis, differentiation and migration (Rosen et al., 2010).

D. Breast Cancer Treatments

1. Overview & Emerging Therapeutic Modalities

Breast cancer treatment varies due to the multitude of cancer types and depending on various factors including the type, stage and grade of the cancer. Surgical treatment is very common for early stage breast cancer patients and it includes lumpectomy or mastectomy. Lumpectomy involves removing cancerous tissue along with the tumor border while mastectomy involves removing the whole breast. Radiation therapy, which employs high energy beams to kill cancer cells, is commonly used post surgery to eradicate any remaining cancer cells in the breast. Systemic therapy is also very common and it involves the use of drugs that travel through the bloodstream to treat cancer cells all around the body. Depending on the type of cancer, systemic therapy varies and different drugs are

administered including chemotherapeutic drugs, targeted drugs and hormonal drugs all of which have a different mechanism of action. Chemotherapeutic drugs work by attacking and killing fast growing cells such as cancer cells. Hormonal drugs work by lowering or blocking the levels of body's natural hormones which sometimes serve to promote cancer growth. Targeted drugs are new and effective since they only target specific molecules in or on cancer cells and often have mild side effects (American Cancer Society, 2015). Breast cancer treatments have developed over the years to include minimally invasive modalities such as cryoablation which treats the tumor through a freezing process (Chandra et al., 2016); laser ablation which treats the tumor through a beam of laser light (Schwartzberg et al., 2016), and ultrasound ablation which is distinguished from other ablation methods in that it is completely non-invasive. These modalities are currently experimental and larger clinical trials need to be performed as ablation techniques may play a significant role in the treatment of breast cancer in the future (Boolbol et al., 2015).

2. Antineoplastic Agents

a. Overview

Cancer chemotherapy involves the use of antineoplastic agents, also referred to as chemotherapy agents, which are injected intravenously or given as tablets through the mouth and can travel through the bloodstream all across the body to kill fast growing cancer cells. The era of chemotherapy started in the early 1940s when Louis Goodman and Alfred Gilman convinced their collaborator, Gustav Lindskog, to use nitrogen mustard to treat a patient with non-Hodgkins lymphoma. Their reasoning was based on autopsy

findings during the First World War, which showed that soldiers were dying of exposure to sulphur mustard gas. Accordingly, Goodman and Gilman performed experiments in mice with lymphoid cancer where they injected a similar agent and observed a striking level of tumor regression which then led them to convince their collaborator to do similarly with the affected patient. Cancer chemotherapy evolved over the years introducing a wide range of drugs including antifolates, alkylating agents, combination chemotherapy and anti-angiogenic agents (Chabner & Roberts, 2005).

Anti-neoplastic agents can be divided into different groups based on their structure and mechanism of action. For instance, anti-metabolites are a group of chemotherapy drugs that obstruct the normal metabolic pathways within cells. Because their structure is analogue to the nucleotide bases, they act at the DNA level and incorporate themselves in the DNA sequence leading to DNA arrest and cell death (Kaye, 1998). Many anti-metabolites have been used in the treatment of solid tumors one is which 5-fluorouracil, a pyrimidine anti-metabolite that is commonly used to treat colorectal cancer (González-Sarrías et al., 2015). Alkylating agents also constitute a class of anti-neoplastic agents and they kill cancer cells by damaging the DNA directly leading to cross linking and mutagenic damage. The repair system and normal base pairing can also be affected among other cellular pathways (Fu et al., 2012). Another class of anti-neoplastic agents is the topoisomerase inhibitors which act by inhibiting the action of topoisomerase enzymes. Under normal status, these enzymes regulate the super coiling of DNA strands which is fundamental to DNA transcription and replication. Thus, the topoisomerase inhibitors would interfere with DNA replication resulting in cell death (Dezhenkova et al., 2014).

b. Types of Chemotherapy drugs

i. Paclitaxel

- *Overview*

Anti-neoplastic agents also constitute mitotic inhibitors which have a different mechanism of action from the classes of chemotherapy drugs mentioned earlier. Based on their mechanism of mitosis inhibition, mitotic inhibitors belong to four different categories; mitosis checkpoint inhibitors, microtubulin enzyme inhibitors, mitosis enzyme inhibitors and microtubulin binders (Tsao & Papadimitrakopoulou, 2011). Paclitaxel, with the trademark "Taxol" belongs to the microtubulin binder's category and was isolated in the early 1960s from the bark of the western yew, *Taxus brevifolia*, hence its name "Taxol" (Wani et al., 1971). It was first approved by the Food and Drug administration (FDA) in 1992 for the treatment of ovarian cancer (Orr et al., 2003) and has been later used to treat other tumors such as breast cancer, lung cancer, liver, and lymphoma (Priyadarshini, 2012).

- *Mechanism of Action*

Paclitaxel is a cytoskeletal drug that inhibits the disassembly of microtubules by stabilizing them. Microtubules are a component of the cytoskeleton consisting of tubulin heterodimers of α and β subunits, the basic structural and "building blocks" of microtubules. Microtubules are important in several cellular processes such as formation of mitotic spindles which are in turn needed for the cell division of M phase. Paclitaxel works by penetrating through the cell and specifically binding to the β tubulin subunit on the inner

surface of microtubules. Paclitaxel locks tubulin by forming a microtubule-paclitaxel complex that prevents microtubules from assembling. This has a major effect on cell function since the shortening and lengthening of microtubules are essential for their function. For instance, chromosomes depend upon this characteristic of microtubules during mitosis since without it; they won't be able to attain a metaphase spindle configuration. Moreover, disruption of microtubule dynamics blocks the progression of mitosis by arresting the cell cycle at the G2/M phase, and eventually leading to apoptosis (Figure 1) (Barbuti & Chen, 2015). Noteworthy, under normal conditions, presence of GTP is required for microtubule polymerization, however; paclitaxel has the capability to polymerize tubulin in the absence of GTP (Orr et al., 2003).

- *Resistance to Paclitaxel*

Despite that Paclitaxel has shown to be an effective anti-cancer drug against several cancers, drug resistance has been limiting its success. Chemotherapy might fail either due to the cancer being innately resistant to the drug and/or to the acquirement of resistance during treatment. Resistance develops based on many factors that are acquired through a series of modifications. To account for this resistance, several possible mechanisms have been proposed for instance, cancer cells can escape the microtubule stabilizing action of Paclitaxel by three ways (Figure 1); over-expression of P-glycoprotein (also termed as ABCB1), a 170 KDa protein encoded by the multidrug resistant (MDR1) gene being one of the major mechanisms of resistance to Paclitaxel (Juliano & Ling, 1976), disruption of both microtubule network and spindle function in cell division by formation

of mutations in both subunits of tubulin, and reduced function of apoptotic proteins such as Bcl-2 and p53 inhibiting the apoptotic response. (Barbuti & Chen, 2015).

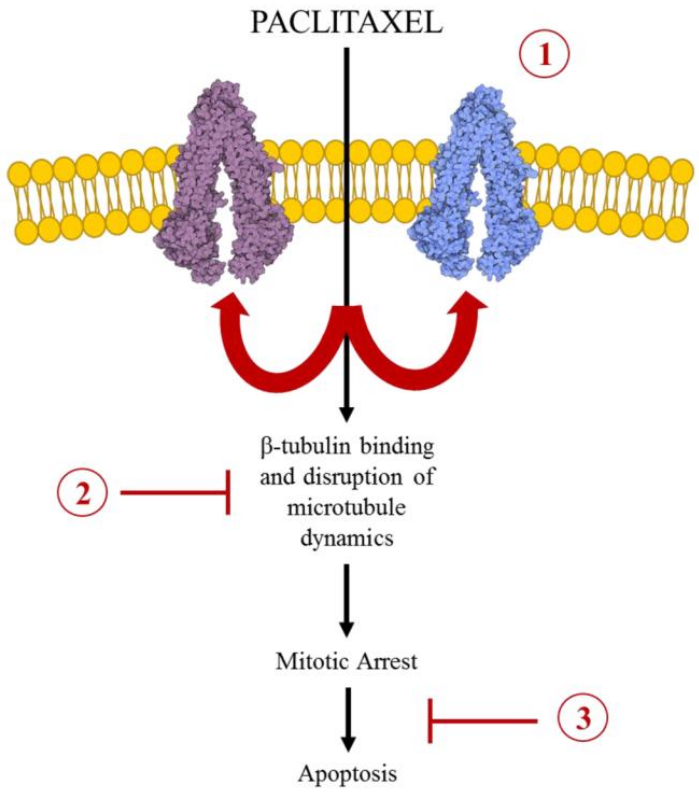

Figure 1: Schematic representation of Paclitaxel's mechanism of action (shown in black arrows) and possible resistance routes (shown in red bars). Paclitaxel penetrates through the cells and binds to β tubulin subunit disrupting microtubule dynamics. This leads to mitotic arrest at the G2/M phase followed by apoptosis. Cancer cells have been found to escape this mechanism by overexpressing transmembrane transporters such as P-glycoprotein (1), mutations in either subunit of tubulin (2) or a reduced function of apoptotic proteins (3) (Barbuti & Chen, 2015).

ii. Doxorubicin

- *Overview*

Doxorubicin, sold under the trade name Adramycin, is a class I anthracylin antibiotic drug isolated by chemical semi-synthesis from a bacterial species, *Streptomyces peucetius,* in the 1960 near the Adriatic Sea (Blum & Carter, 1974). It is used to treat a variety of cancers including breast, cervical, prostate, lung, bone and thyroid (Tacar et al., 2013).

- *Mechanism of Action*

Doxorubicin works by intercalating DNA and interfering with macromolecular biosynthesis (Perez-Arnaiz et al., 2014). This intercalation leads to the inhibition of one of the main enzymes, Type II Topoisomerase, which catalyzes the unwinding of DNA for transcription. After the enzyme has broken the DNA chain for replication, doxorubicin stabilizes it and hence prevents the DNA helix from being released preventing DNA replication and initiating DNA damage. When the attempts to repair DNA damage fail, apoptotic response is triggered and cellular growth is hindered at G1 and G2 phases (Rivankar, 2014). Doxorubicin has also shown to inhibit the primary DNA methyltransferase responsible for DNA methylation in mammalian cells, DNA methyl transferase 1 (DNMT1), in human colon cancer cells. Interference with the function of DNMT1 leads to chromosomal instability, transcriptional deregulation and apoptotic cell death (Yokochi & Robertson, 2004). Other doxorubicin actions include the production of

free radicals which leads to further DNA damage and macromolecular inhibition, and this is considered partially responsible for the cytotoxicity of the drug (Tacar et al., 2013).

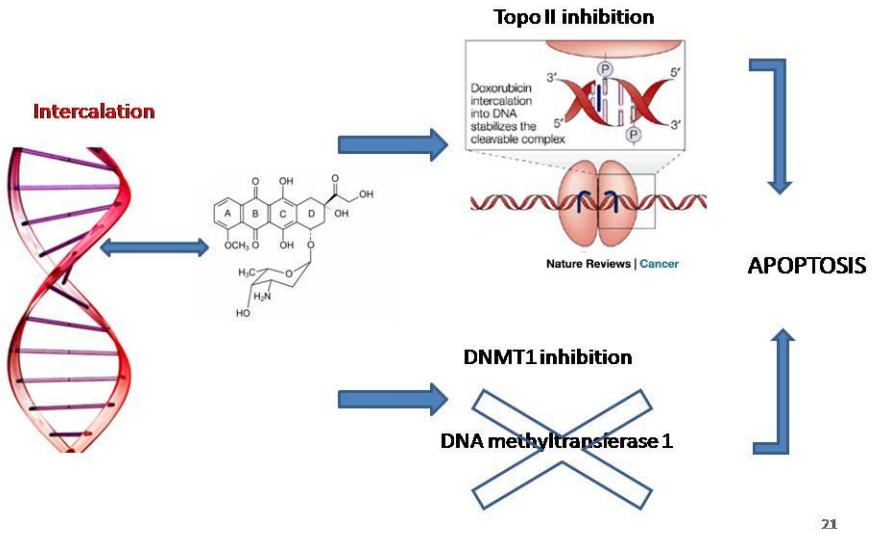

Figure 2: Schematic illustration of Doxorubicin's mechanism of action. Doxorubicin intercalates into DNA and inhibits topoisomerase II by stabilizing the cleavable complex. In addition, doxorubicin inhibits DNA Methyl Transferase1. Both actions will therefore lead to apoptosis. Figure is amended from Lee et al., 2004; Younes, MSc, Thesis 2015.

- *Resistance to Doxorubicin*

Similarly to Taxol, Doxorubicin resistance is limiting its success. Doxorubicin resistance has been observed in a number of cancer cells including melanoma cells where it has been shown that doxorubicin resistance doxorubicin resistance is mediated by the ABC transporter, ABCB8, by protecting the genome of the mitochondria. Moreover, the

knockdown of this ABC transporter with shRNA showed a decrease in doxorubicin resistance by 3-4 folds (Tacar et al., 2013). MDR phenotype, which involves over-expression of multidrug transporters such as P-glycoprotein, is one of the recognized mechanisms of drug resistance in cancer cells. Caveolin-1 protein has been shown to affect the MDR phenotype on cell membrane by hindering the entrance of drugs to the cells and thus playing a role in resistance to doxorubicin (Raghazan & Shajahan, 2014). It has been shown that a cav 1 mutant in cancer cells obstructs the interaction with P-glycoprotein and eliminates the inhibition of P-glycoprotien by Cav-1(Lee et al., 2016).

3. Combination Therapy

a. Overview

Breast cancer is a heterogeneous group of neoplasm's where each case is considered different and thus each patient will have a unique method of treatment based on several characteristics including the size of the cancer, probability of recurrence, and the general health of the patient. Resistance is a limiting factor for the success of cancer treatments and hence decreasing the likelihood that it will develop is essential to improve survival rates. For that reason, combination therapy is currently used. Combination therapy could involve the use of more than one treatment method and depending on the combination of treatment methods used, adjuvant and neoadjuvant therapies are given where the former refers to a therapy that is given after the main treatment and the latter refers to therapy that is given before the main treatment. For instance, it is common that in early stage breast cancer patient's surgery is performed followed by chemotherapy,

radiation therapy and hormonal therapy. In some cases, systemic therapy could be given prior to surgery in order to shrink the size of the tumor and increase the success rate of the surgery. Moreover, combination therapy could also involve the use of more than one chemotherapy drug or more than one hormonal drug because each drug employs a distinct mechanism of action and so this will decrease the probability of resistance occurring later on (American Cancer Society, 2015). The addition of pertuzumab, a drug that attaches on the HER2 to the treatment regimen, trastuzumab and docetaxel, has shown to improve the survival of the patients when compared with the addition of placebo in HER2+ breast cancer patients (Swain et al., 2015). The addition of palbociclib, a drug that targets cyclin-dependent kinase (CDK) 4 and CDK6 to letrozole, an aromatase inhibitor improved progression-free survival in women with advanced oestrogen receptor-positive and HER2-negative breast cancer (Finn et al., 2015).

b. Standard Therapy in Combination With Experimental Therapy

Some therapies are currently experimental and are being tested in combination with standard therapy. For instance, High intensity focused ultrasound (HIFU) in combination with chemotherapy can lead to a better outcome. In one study, HIFU combined with chemotherapy showed to be safe and promising method in treating patients with hepatoblastoma (Wang et al., 2014). In another study, multi drug resistant breast cancer cells were diminished in 4 days when the combination of HIFU and low dose chemotherapy drug, Docetaxel was used (Vo et al., 2015). Moreover, the combination of

HIFU and radiotherapy has shown to improve symptoms and quality of life in patients with locally advanced pancreatic carcinoma (Li et al., 2016).

4. High Intensity Focused Ultrasound

a. Overview

High Intensity Focused Ultrasound (HIFU) is an ex-corporeal medical device that was first introduced in the 1940s for the treatment of neurological disorders (Lynn et al., 1942) and has been subjected to several improvements since then. It is a non-invasive and non-ionizing therapeutic method that can be utilized to treat a variety of solid tumors such as liver, prostate, breast, pancreas and kidney by destroying tissues that are deep inside the body (Maloney & Hwang., 2015). HIFU use is applied widely in Asia and in certain parts of Europe, but it has only been approved in the USA by the FDA for prostate tissue ablation (Book, 2015) and still pending approval for treatment of other organs. Because HIFU is a non-invasive procedure, the risks that are linked with invasive procedures are minimized since there is no need for transfusions or incisions in ablating the tumor. In addition, since HIFU is not associated with any ionizing radiation, the numbers of sessions are not limited and the treatment could be performed with the patient under several conditions whether fully conscious or lightly sedated. Moreover, HIFU could serve as an alternative treatment method for patients who do not have any other options available (Zhou, 2014). Moreover, there is a major difference between the shape of the HIFU transducer and that of the ordinary transducer. The shape of an ordinary ultrasound transducer is flat or convex thereby allowing the ultrasound waves to diverge, thus

dispersing their intensity. On the other hand, the shape of a HIFU transducer is concave allowing it to focus its high power on the focal spot resulting in tissue ablation (Figure 3).

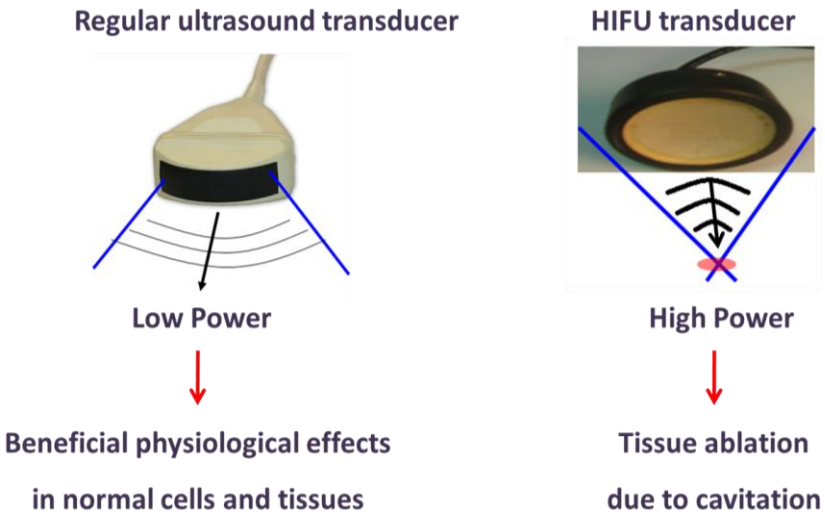

Figure 3: A schematic representation showing the difference between the shape of an ultrasound transducer and a HIFU transducer. Figure amended from Malkhasian L, MSc Thesis 2012.

b. Biological and Mechanical Effects of HIFU

When HIFU operates at low intensities, it causes slow heating by which the tissue of interest is exposed and subjected to a direct increase in temperature by a few degrees above the normal body temperature. On the other hand, when HIFU operates at high intensities, a phenomenon termed cavitation will occur (Prasanna et al., 2008). Cavitation is referred to as the formation and destruction of bubbles which occurs when there is an alteration in the pressure of the liquid. When the pressure of the liquid becomes low, cavities are formed and bubbles will expand resulting in tissue damage. This effect is seen in tissues specifically at the focal spot. Noteworthy, cavitation can be attained through

the spontaneous formation of microbubbles under the influence of the high intensity ultrasound waves or it can be stimulated by exogenous application of microbubbles (Phenix et al., 2014). In the focal spot, cell death occurs by necrosis since HIFU employs a concave shaped ultrasound transducer that gives intensified energy which is focused at the target tissue. The surrounding tissue is believed to be left unharmed (Rove et al., 2010).

i. Sonoporation

Mechanical effects of cavitation can alter the permeability of cell membranes by the formation of temporary pores, a process referred to as sonoporation (Uemura et al., 2015). Formation of transient pores start to form when the cell membrane is disrupted by the expansion or collapse of the bubbles which produce forces around the cell membrane allowing molecules, otherwise impermeable, to get inside the cell resulting in increased membrane permeability (Figure 4). Depending on the presence or absence of microbubbles, the size of the pores varies from few nm to few μm. Studies demonstrated that the pore size increases with increasing experimental parameters such as acoustic pressure, sonication time and duty cycle. Furthermore, it has been shown that as the pore size increases, the cell viability decreases (Zhou et al., 2012). In addition, sonoporation has been reported to impact the structure of organelles (Zeghimi et al., 2012). Sonoporation is still under extensive research and it is being investigated as a novel approach for gene or drug delivery.

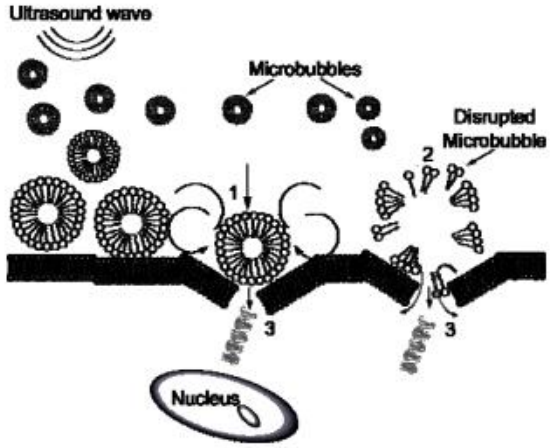

Figure 4: Schematic representation of the mechanism of sonoporation. Transient pores start to appear on the cell membrane when the bubbles are expanding and/or collapsing generating a force around the membrane causing the agents to go through the pores into the cells (Phenix et al., 2014).

ii. Sonoporation and Cancer

Pre-clinical studies have shown that sonoporation could be used to enhance the uptake of drugs into cells and reduce tumor burden. A clinical trial has shown that ultrasound in combination with microbubbles and chemotherapy can improve the uptake of chemotherapy drugs and can also increase the number of chemotherapy cycles since the drugs are released in a targeted location increasing local drug concentration (Kotopoulis et al., 2014). Another study where the combined effect of ethanol and HIFU was investigated and found synergistic in the ablation of liver tissue and liver cancer cells, the rate of diffusion of ethanol was increased due to HIFU induced sonoporation (Hoang et al., 2014). To study sonoporation, fluorescent labeled molecules with different localization profile depending on their molecular size are used. For instance, dextran molecule with a size of 3 KDa diffuses into the cytosol and into the nucleus while a dextran molecule of size 70 kDa

was found only in the cytosol. Larger molecules of dextran with sizes over 150 KDa were observed as patchy structures in the cytoplasm (Meijering et al., 2009).

iii. Biomedical Applications of HIFU

Generally, exposure levels of ultrasound could be varied resulting in diverse effects in their therapeutic outcome. When ultrasound is operated at a low power, beneficial biological effects may be produced while at high power; cells die due to irreversible necrosis. Therefore, ultrasound therapy is divided into "low power" and "high power" applications used for distinct purposes. Low power applications encompass physiotherapy, bone healing, and sonopheresis among others; while high power applications include the use of HIFU which has both thermal and mechanical effects. Apart from the use of HIFU in cancer therapy, it also used to treat vascular occlusion and haemostasis (Ter Haar, 2007). In addition, HIFU has been shown to be effective in reducing intraocular blood pressure in patients with refractory glaucoma (Melamed et al., 2015).

c. HIFU treatment

i. In cancer

The use of HIFU for tumor ablation has significantly improved over the years and this is because of the advances in imaging methods such as magnetic resonance imaging (MRI) and transducer technology. HIFU technology has developed to be a promising approach for the treatment of certain types of cancer including liver tumors where it has been shown to be safe and practical in a panel of 31 patients whom were employed into two ethically approved clinical trials (Leslie et al., 2012). HIFU has also shown to ablate a targeted spot of the pancreas without damaging the nearby tissue (Wu,

2014). HIFU has been applied to treat other tumors such as brain, kidney (Cranston, 2015) soft tissue sarcoma, breast, and bone tumors (Orsi et al., 2016). Its use has also been shown to be favorable in the treatment of prostate cancer where it resulted in almost complete ablation of the prostate gland (Nomura & Mimata, 2012). Furthermore, technical, imaging and technological advancements in HIFU have shown to improve clinical outcome in patients with prostate cancer (Uchida et al., 2015).

ii. In Breast Cancer

Though surgery is the standard method of treatment for breast cancer, some patients may not wish to undergo surgery because of the complications it might result in or because the cosmetic outcome isn't so satisfactory. Since HIFU is a non-invasive technique, it might serve as an alternative option for many and might potentially result in a decreased risk of complications and an improved cosmetic result. The use of HIFU for breast cancer ablation has emerged over the years since it can be used in parallel with MRI (Marincola et al., 2014). Not only does MRI provide guidance, exceptional anatomical imaging and real-time monitoring of temperature but it is also fundamental to monitor the procedure of the treatment and confine the target area.

In 2001, a group of scientists described the first MRI-guided HIFU system to treat an invasive breast cancer patient showing that the therapy is feasible and effective (Huber et al. 2001). Other groups demonstrated a similar platform and showed that by means of MRI, HIFU treatment is a promising procedure for the treatment of invasive lobular and invasive ductal carcinoma. Nonetheless, minor skin burns resulted as a

complication in a few of the patients (Furusawa et al. 2006; Gianfelice et al. 2003). Moreover, a recent study published in 2016 described a MRI-guided HIFU platform where the breast is targeted laterally reducing the risk of unintended exposure to other organs next to the breast. In this study, 10 patients with invasive breast cancer underwent treatment and demonstrated a safe outcome in addition to proven necrosis (Merckel et al. 2016).

E. Caveolae and Caveolins

1. Overview of Caveolae and Caveolins

Caveolae were first described in the cell membrane by electron microscopy around 60 years ago by Palade in blood capillaries and by Yamada in the gall bladder epithelium and were described in nearly all cell types ever since (Palade, 1953; Yamada, 1955). Caveolae are defined as non-clathrin coated membrane invaginations that are 50-100nm wide composed of mainly cholesterol and sphingolipids (Figure 5A). They are found in most cell types but primarily abundant in endothelial cells, adipocytes and muscle cells. Caveolae play a central role in endocytosis, transcytosis, and have several functions in signal transduction. The major structural proteins of caveolae formation are members of the caveolin protein family. In vertebrates, the caveolin gene family consists of *cav-1*, *cav-2* and *cav-3* genes, encoding for the proteins caveolin-1 (Cav-1), caveolin-2 (Cav-2), and caveolin-3 (Cav-3) respectively. Caveolae formation is defined mainly by the expression of caveolin-1 protein (Figure 5B) (Kiss et al., 2012).

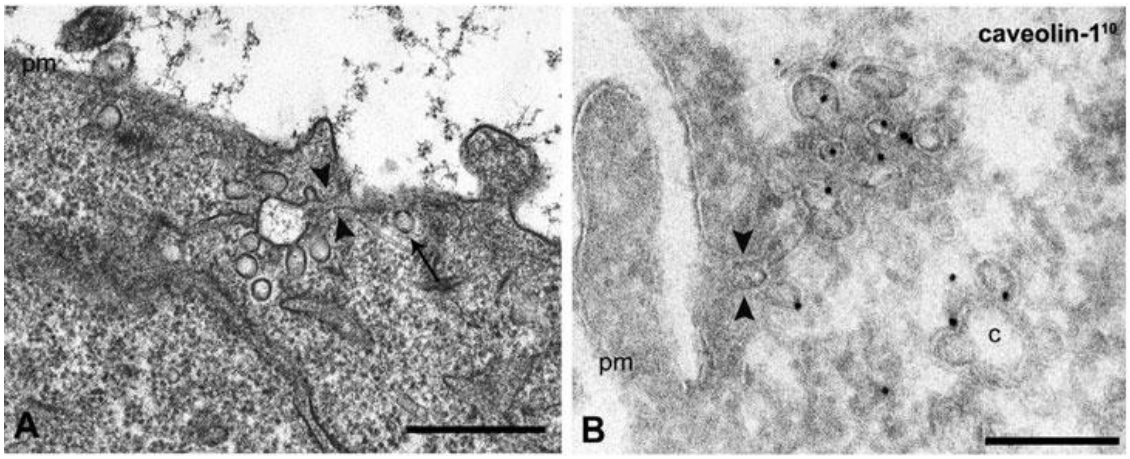

Figure 5: Transmission electron micrographs of the structure of caveolae. Panel on the left (A) shows how the caveolae are connected to the membrane by invaginations and panel on the right (B) shows immunolocalization of Cav-1 protein at caveolar sites (Modified from Kiss, 2012).

After the caveolin proteins are produced in the endoplasmic reticulum (ER), they start to oligomerize and are then transported to the Golgi apparatus that interact with cholesterol to form a stable caveolin domain (Hayer et al., 2010). Thus, all three caveolin proteins are linked with membranes including the plasma membrane, Golgi apparatus and endoplasmic reticulum. Moreover, all caveolin proteins are small integral membrane proteins inserted into the caveolar membrane with a formation of a hairpin structure when inserted into the cytoplasmic leaflet of the membrane bilayer and with both the amino and carboxyl termini facing the cytoplasm (Figure 6). Cav-1 is expressed in almost all cells but mainly with high levels in adipocytes, fibroblasts and endothelial cells. Caveolin-2 can't bind to cholesterol without interacting with caveolin 1 since it has been shown that it co-localizes with caveolin-1. This in support of other studies that indicates that caveolin-2 is an accessory protein to caveolin-1. Unlike caveolin-1 and caveolin 2 which are expressed in most cell types, caveolin-3 is specific to muscle cells. Besides, caveolin-3 does not require

caveolin-1 to drive caveolae formation. Moreover, caveolin-1 and caveolin-2 form stable hetero-oligomers while caveolin-1 and caveolin-3 can form homo-oligomers. (Kiss et al., 2012)

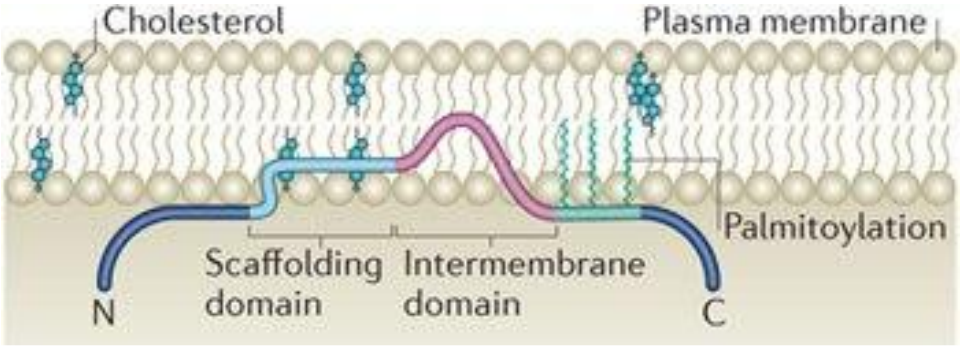

Figure 6: Schematic representation showing the organization of caveolins. Caveolins are integral membrane proteins with putative hairpin loop structures embedded within the membrane and both the amino-terminus and carboxyl-terminus in the cytoplasm (Modified from Parton & del Pozo, 2013).

2. Caveolin-1

a. Overview

Caveolin-1 protein is encoded by *cav-1* gene located on chromosome 7. It is a 22 KDa protein consisting of 178 amino acids. Two isoforms exist for caveolin-1 protein, termed α and β. They are possibly generated by alternative splicing from two distinct mRNAs at least in some cell types signifying the presence of a transcriptional control over both isoforms. Both isoforms are identical except for the presence of 31 additional amino acids at the N terminus of α isoform (Kogo et al., 2004). This difference results in a 24 kDa Cav-1 α with 178 amino acids, opposed to a 21 kDa Cav1-β with 148 amino acids. Accordingly, the Cav-1 α is considered a slower migrating species than the faster Cav-1 β

isoform. Moreover, Cav-1β lacks a tyrosine (Y) phosphorylation site at residue 14 which is present in cav-1 α. Src kinase phosphorylates Cav-1α at the tyrosine residue 14 (Y14) of its N-terminus. Phosphorylation at this amino acid leads to protein buildup at focal adhesion sites and consequent signal transduction (Hehlgans and Cordes, 2011). Additionally, some cysteine residues in the C-terminal domain of Cav-1 are S-acylated by palmitoylation (Parton et al., 2006).

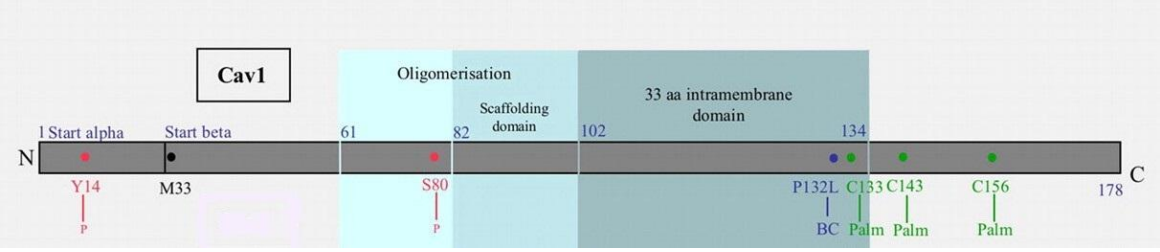

Figure 7: Schematic representation showing the domain organization of CAV1 protein. Post-translational modifications and disease-associated mutations are represented. Palmitoylation (Palm) sites in CAV1 are pointed out in green, a Tyr phosphorylation site (Y14) in red, and the starting methionine (M33) of CAV1β is shown in black. Disease-associated amino acid substitutions in CAV1 are shown in blue. P132L is a common mutation in CAV-1 resulting in breast cancer (BC) (Modified from Parton et al., 2006).

b. Role in Cancer

The relationship between cav-1 and its role as a tumor suppressor or a tumor promoter remains one of the most controversial areas in science. The most likely explanation for this discrepancy is tumor stage dependency and the cellular environment. Supporting the notion that cav-1 functions as a tumor suppressor, a study has shown that mRNA and protein levels of cav-1 were down-regulated in oncogene transformed fibroblasts in culture (Koleske et al., 1995). Re-expression of cav-1 in these cells resulted in a reverted transformed phenotype and prevented anchorage independent growth (Engelman

et al., 1997). Moreover, the expression of cav-1 was shown to be down-regulated in several tumor entities including human ovarian carcinoma (Weichen et al., 2001) and in colorectal cancer where loss of stromal cav-1 expression was associated with poor prognosis (Zhao et al., 2015). On the other hand, other reports have shown that cav-1 was over-expressed in different types of cancers including prostate, pancreas, esophageous and non-small cell lung carcinoma (Hehlgans & Cordes, 2011). In pancreatic cancer, Cav-1 was overexpressed in human pancreatic cell lines, mouse models, and human pancreatic tumors, and was associated with poorer tumor grade and clinical outcomes (Chatterjee et al., 2015). Taken together, these studies suggest that Cav-1 is implicated in both tumor suppression and oncogenesis.

c. Role in Breast Cancer

Cav-1 has also shown to have a controversial role during breast carcinogenesis. Cav-1 was shown to be down-regulated in a series of breast cancer cell lines when compared to normal epithelial cell lines. Cav-1 expression in MCF7 and T47D breast cancer cell lines greatly reduces tumor cell growth and tumorigenicity in soft agar (Lee et al., 1998). In addition, transfection of cav-1 gene into MCF7 breast cancer cell line showed reduced cell proliferation and cell viability when compared to the vector control transfectants (Hino et al., 2003). In vivo studies showed a faster tumor formation in mice lacking Cav-1 expression (Ciocca et al., 2012). As for human studies, cav-1 expression was shown to be low in invasive lobular carcinomas and invasive ductal carcinomas by microarray analysis and immunohistochemistry (Weigelt et al., 2010). On the other hand, several lines of evidence have been shown *in vitro* and *in vivo* suggesting an oncogenic

function for cav-1. Caveolin-1 expression in the Hs578T cell line positively correlated with the number of colonies and colony size in soft agar and reduced apoptosis (Wu et al., 2007). In addition, overexpression of cav-1 was observed in metastatic or deceased patients in a study done on 930 breast cancer patients (Garcia et al., 2007).

3. Caveolin- 1 and Caveloe-Dependent Endocytosis

Caveolae are considered a sub domain of glycolipid rafts (Anderson, 1998) but because its formation is associated with cav-1, it is considered to have a different internalization pathway than that of rafts. Nonetheless, they do share fundamental similarities in their pathways which are defined by their clathrin independence, dynamin dependence, and sensitivity to cholesterol diminution (Nabi & Le, 2003).

In accordance with that cav-1 is crucial in the formation of caveolae, it has been shown that few to no caveolae are present in cells in which cav-1 expression is significantly diminished or absent and that re-introduction of cav-1 into these cells resulted in the re-formation of caveolae at the plasma membrane (Fra et al., 1995). Noteworthy, oligomerized caveolin and associated proteins and lipids allow caveolae to form a stable functional unit at the cell surface. Caveolae have the ability to stay at the cell membrane for a long period of time and their internalization can be triggered by various agents including Simian Virus 40 (SV40) virus which is the one of the most extensively studied ligands for caveolar endocytosis. SV40 virus has shown to be internalized specifically through caveolae-dependent endocytosis because when clathrin dependent endocytosis was

inhibited by expressing a dominant negative mutant of the EGF receptor pathway substrate 15 (Eps15), endocytosis of SV40 was not affected. SV40 serves as a model ligand not only because it has many advantages but mainly because it is well identified in terms of structure and composition. SV40 is recruited to the plasma membrane by histocompatibility (MHC) class 1 antigens after which it diffuses down the membrane till it becomes trapped in caveolae for about 20 minutes. This is followed by caveolae and virus pinching off the cell membrane and moving as caveolin-coated endocytic vesicles into the cytoplasm. Binding of the SV40 to caveolae triggers a signal transduction cascade that has many effects including protein tyrosine phosphorylation and actin depolymerization. Phosphorylation of tyrosine residues by one or more tyrosine kinases occur within the caveolae. Afterwards, actin is sequestered to the virus loaded caveolae forming an actin patch. Subsequently, dynamin is also sequestered to the site but remains for a short period of time after which a burst of actin polymerization occurs on the actin patch. All of these changes are shown to be necessary for the formation and internalization of caveolar vesicles. Virus loaded caveolae vesicle is now released from the cell membrane and is internalized into the cytosol (Figure 8) (Pelkmans et al., 2002). Loaded caveolae vesicle now transports its cargo to a larger complex endosomal compartment termed caveosome. Caveosome have a neutral pH and a membrane rich in cholesterol and glycosphingolipids. Interestingly, caveosomes do not collect cargo endocytosed via clathrin-coated pits. During collecting the cargo from the caveolae vesicles, caveosomes become ever more dynamic and collect the cargo to the ER (Pelkmans et al., 2001).

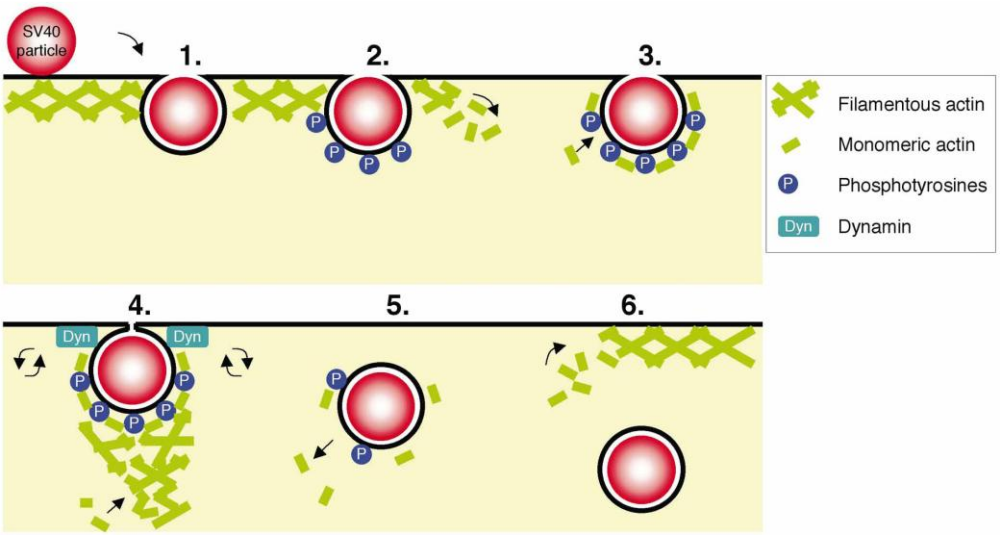

Figure 8: Schematic representation showing the early stages of SV40 internalization by caveolae. SV40 virus passes through the membrane and gets trapped in caveolae which are associated with the actin cytoskeleton (1). This binding triggers a signal transduction event leading to protein tyrosine phosphorylation and actin depolymerization (2). Monomeric actin is sequestered to the membrane forming an actin patch (3). This is followed by recruitment of dynamin and a burst of actin polymerization that acts on the actin patch (4). Virus loaded caveolae are now internalized into the cytosol (5) after which the actin cytoskeleton returns to its normal pattern (Pelkmans & Helenius, 2002).

Other ligands could also be internalized by caveolae-dependent endocytosis including cholera toxin (Montesano et al., 1982) and serum albumin (Schnitzer et al., 1994). Moreover, other viruses enter cells by this route including polyoma virus where it was shown to enter mouse cells (Richterova et al., 2001). Noteworthy, common inhibitors of caveolae-dependent endocytosis include filipin and genistein (Rejman et al., 2005). Genistein which is commonly known to be present in soy beans is a phytoestrogen that belongs to the category of isoflavones and was isolated in 1899 from Dyer's broom (Genista tinctoria) (Perkin & Newbury, 1899). Genistein is a common inhibitor of tyrosine

protein kinases mostly of epidermal growth factor receptor (EGFR) and an inhibitor of caveolae pinching. It has been shown that it inhibits SV40 infection and SV40-induced alterations in the actin cytoskeleton (Pelkmans et al., 2002).

F. Gap in Knowledge, Rationale, and Hypothesis

In previous studies in our laboratory (Lori Malkhassian MSc Thesis 2012; Ingrid Younes MSc Thesis 2015), we examined the alterations in mechanotransduction due to changes in the physical properties resulting from the exposure of MDA-MB-231 breast cancer cells and MCF-10A immortalized mammary epithelial cells to ultrasonic waves from a custom-designed HIFU setup and we looked at the resultant consequences on cellular response to anti-neoplastic agents. We assessed the *in vitro* effects of sub-lethal HIFU exposure on the expression of seven mechanosensitive genes namely *CAV-1* (Caveolin-1 α & β), *Hic-5* (Hydrogen Peroxide-Inducible Clone 5), *PXN* (Paxillin), *TTLL4* (Tubulin-Tyrosine Ligase-Like Protein 4), *TWIST1* (Twist-Related Protein 1), *CTSD* (Cathepsin D), and *HSPA1A* (Heat Shock Protein 70) whereby we quantified significant enhanced expression of *CAV-1α, PXN*, and *Hic-5* that was immediate-early in MCF-10A cells and delayed in MDA-MB-231 Cells. Additionally, we noted a significant immediate - early transient increase in *TTLL4* expression in both cell lines and in *TWIST1* expression in MDA-MB-231 cells. Notably, sub-lethal HIFU exposure had no significant effect on the expression of *CAV-1*(total pool; i.e. combined pool of α and β isoforms), *CTSD*, and *HSPA1A* in both cell lines. Moreover, sub-lethal HIFU exposure of cells at 6hr or 30hr prior to the *in vitro* addition of anti-neoplastic agents sensitized MDA-MB-231 and MCF-

10A cells to sub-cytotoxic doses of Taxol (1.5nM, 7.5nM) and Doxil (0.05µM, 0.5µM) when tested over a period of four days. Furthermore, MDA-MB-231 cells surviving single or dual rounds of HIFU exposure at the focal spot and passaged over 3-to-6 weeks in tissue culture showed no significant change in their *in vitro* sensitivity to Taxol or Doxil (paper in preparation).

Given that sub-lethal HIFU exposure sensitizes MDA-MB-231 cells to sub-cytotoxic doses of Taxol and Doxil, we are next interested in deciphering the mechanisms that are implicated in this enhanced *in vitro* sensitivity of MDA-MB-231 to anti-neoplastic agents in order to provide mechanistic insight into the results previously obtained in our laboratory. With reference to the above, **we hypothesized that sonoporation and caveoloe-dependent endocytosis are implicated in the enhanced sensitivity of MDA-MB-231 cells post sub-lethal HIFU exposure.**

G. Objective of the Study and Specific Aims

The objective of this proposed research study is to identify the mechanisms that are implicated in the enhanced *in vitro* sensitivity of MDA-MB-231 cells to sub-cytotoxic doses of Taxol and Doxil post sub-lethal HIFU exposure. The proposed study is comprised of two main specific aims subdivided:

Aim 1 – To determine if sonoporation is implicated in the enhanced *in vitro* sensitivity of MDA-MB-231 cells to sub-cytotoxic doses of Taxol and Doxil post sub-lethal HIFU exposure. Specific tasks include:

Performing FITC-dextran uptake assay in mock-treated controls versus HIFU-treated MDA-MB-231 cells followed by flow cytometry acquisition and microscopic observation. Digitonin treatment will be used as a positive control for FITC-dextran uptake in cells.

Aim 2 – To determine if caveolae-dependent endocytosis is implicated in the enhanced *in vitro* sensitivity of MDA-MB-231 cells to sub-cytotoxic doses of Taxol and Doxil post sub-lethal HIFU exposure. Specific tasks include:

Applying Genistein as an inhibitor of caveoloe-dependent endocytosis to check if it is implicated in the enhanced *in vitro* sensitivity. For this aim, two sub-cytotoxic doses were applied for each of Taxol and Doxil. Afterward, the cells that were subjected to sub-lethal HIFU exposure were then seeded at a density of 20, 000cells/well in 96-well plates. Genistein was then added to the cells after 6 hours and 30 hours. Genistein was then discarded from the cells and the chemotherapy drugs were added at the 6 hr time point and the 30hr time point. Viable cells were then counted using the trypan blue vital stain exclusion assay daily, over a period of 4 days.

CHAPTER II

MATERIALS AND METHODS

A. Cell Culture

1. MDA-MB-231

MDA-MB-231 is a human breast adenocarcinoma cell line that was kindly provided by the laboratory of Dr. Rabih Talhouk. This cell line is maintained and propagated using specialized media consisting of *Roswell Park Memorial Institute* RPMI 1640 (Lonza), supplemented with 1% Penicillin-Streptomyocin (Lonza) and 10% Fetal Bovine Serum (FBS) (Sigma-Aldrich). The doubling time of these cells is about 26 hours. When a confluent density of 80% is reached, cells are washed with 5 ml of 1X Phosphate Buffered Saline (PBS) without Ca and Mg (Lonza). Cells are then trypsinized with 1 ml of 2×Trypsin (Lonza) and incubated for 30 seconds in a 37°C CO_2 (5%) incubator. Post incubation, cells are detached from the surface of the plate to then be neutralized with an adequate amount of media and be centrifuged at 600xg at 4°C for 5min. Post centrifugation, the pellet is re-suspended with 1ml of complete growth media. An appropriate volume of cells is distributed in the tissue culture plates that are pre-filled with 10ml of complete growth media.

B. HIFU Experiments

1. Cell Preparation pre-HIFU

At 80% confluence, MDA-MB-231 cells are trypsinized and centrifuged as previously mentioned, then distributed over 0.2ml PCR tubes with a density of 2×10^5 cells in each tube (depending on the number of PCR tubes needed for the experiment, the number of plates of cells prepared is varied). After preparation, the tubes are placed in a thermostatic container and transferred to the Mechanical Engineering Department at AUB, where the HIFU cell suspension setup is located (Figure 9). The tubes are then immersed through their adequate holders in 37°C degassed, double distilled water, ready to be exposed to HIFU. The HIFU experimental conditions are: i) cells exposed at the focal point; 100%, ii) cells exposed to residual HIFU (i.e. sub-lethal exposure that is not at the focal spot; 25.7%), iii) cells immersed in the tank without being subjected to any exposure (mock control). The different experimental parameters used are as follows: Volts: 256Vpp, frequency: 500KHz, temperature of water tank: 37°C, duty cycle: 2%, sonication time: 10msec, and total exposure time: 200msec

2. Cell Re-suspension and Seeding Post-HIFU

Post HIFU exposure, MDA-MB-231 cells are diluted and re-suspended with their appropriate media ready to be seeded at two different densities for different sets of experiments. The first set of experiments involves seeding the cells at a density of 72 $x10^{4/}$4000µl (4 tubes) in each well in a 6 well plate to have sufficient number of cells for

analysis. The second set involves seeding the cells at a density of $2x10^4$/100µl cells in each well in a 96-well plate. Cells are then placed in a 37°C CO2 (5%) incubator.

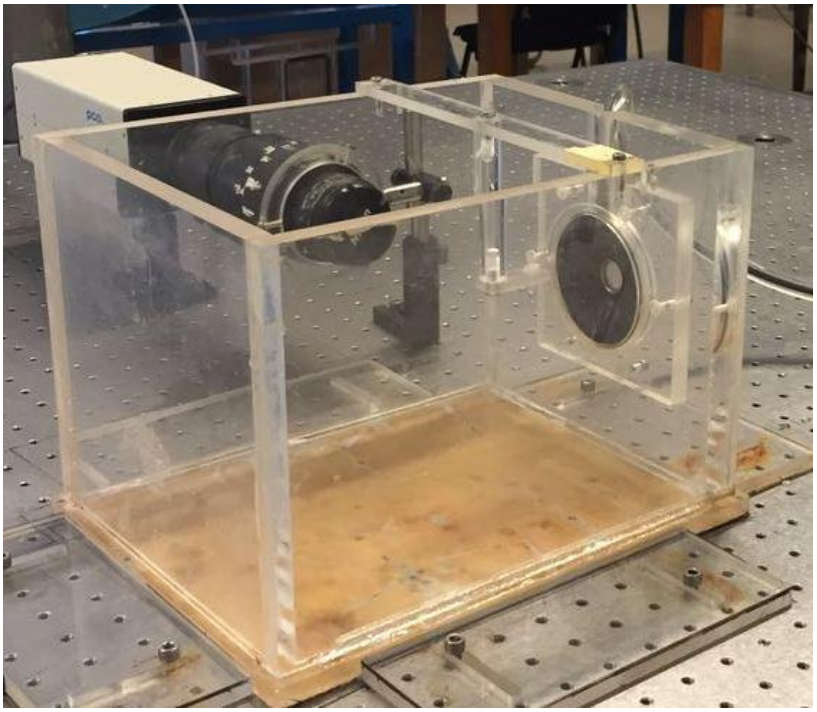

Figure 9: A photographic image of the HIFU cell-suspension setup (Courtesy of the laboratory of Dr. Ghanem Oweis, Department of Mechanical Engineering, FEA, AUB).

C. Assessment of FITC-Dextran uptake

1. Flow Cytometry

Post HIFU exposure, MDA-MB-231 cells are seeded at a density of 72 $x10^{4/}$4000µl per well in a 6 well plate for two time points (6 hours and 30 hours). At the respective time point, media is discarded and cells are washed once with 2ml of PBS (1X). FITC-Dextran (Sigma, Cat. # 46945-100MG-F), a fluorescent marker used to determine sonoporation, is then added at a concentration of 7.7 mg/ml (prepared in incomplete media;

i.e. without FBS) to the cells for 1 hour. Cells are then washed twice with 2ml of PBS (1X) for 2 minutes. Post washing, cells are trypsinized and centrifuged as previously mentioned at 600xg at 4°C for 5min. The cell pellet is washed once with 3ml of PBS (1X), then centrifuged again at 600xg, 4°C, for 5min. The cell pellet is then fixed with 4% PFA solution (Paraformaldehyde, Electron Microscopy Sciences) and homogenized for 20 minutes at room temperature. Cells are then centrifuged at 600xg at 4°C for 5min and the cell pellet is rinsed once with 1ml of PBS (1X) post fixation. Cells are re-centrifuged and the cell pellet is finally re-suspended in 500µl of PBS and transferred to a BD Falcon 5ml polystyrene round-bottom tube (BD Biosciences REF: 352058) to be taken for flow cytometry data acquisition. Digitonin (Sigma Aldrich- D141) is used as a positive control to make sure that the cell membrane is permeabilized indeed to allow dextran uptake. It is used at a concentration of 20µM for 10 minutes.

2. Microscopic Imaging

FITC-dextran assessment by fluorescence microscopy is similar to the protocol designed for flow cytometry except that the cells are seeded on coverslips. Post fixation and washing steps, the coverslips are mounted on slides using UltraCruz™ Hard-set Mounting Medium (Santa Cruz Biotech. Inc., sc-359850) based on manufacturer's specifications. They are sealed with nail polish and stored at 4°C for microscopic imaging. Image acquisition was performed within 24 to 48hrs of staining using the LSM710 Confocal Microscope (Carl Zeiss, DTS facility, AUB) of both FITC-Dextran and DAPI using the 63x/ 1.40 oil DIC M27 objective magnification. Eight frames were acquired per

slide with the 60X objective while three frames were acquired for the negative control. Cells were first examined with a standard phase-contrast microscope (Olympus microscope, Axiovert 200, Zeiss, CRSL facility, AUB) to assess overall confluence and spreading of cells.

D. Assessment of Caveoloe-Dependent Endocytosis.

Post HIFU exposure, cells are seeded at a density of $2x10^4$/100µl cells per well in a 96-well plate for two time points (6 hours and 30 hours). These cells are cultured for 4 time points, once per 24 hr increments.

1. Preparation of Genistein

Genistein (Sigma, G6649-25MG) is a chemical inhibitor of caveolae-dependent endocytosis and is diluted with Dimethyl Sulfoxide (DMSO). It was added at a concentration of 100µM to the cells either six or thirty hours post seeding for 30 minutes. A series of dilutions is prepared to obtain the specific concentration.

2. Preparation of Anti-neoplastic agents

Working concentrations of each of Taxol (Sigma, T7402) and Doxil (Sigma, D1515) were prepared to be added to the cells after discarding Genistein. The chosen concentrations for Taxol are 1.5nM and 7.5nM while for Doxil, we used 0.05µM and 0.5µM. Taxol was diluted with Dimethyl sulfoxide (DMSO) while double distilled water was used for Doxil based on manufacturer's specifications and preparation instructions.

E. Viability Assay

1. Microscopic Observation (Phase-Contrast)

Cells, post HIFU and Genistein/chemo addition and prior to counting for the 4 days, were examined by microscopic observation using a standard phase contrast microscope with a 40x magnification to exclude any potential artifact or contamination.

2. Trypan Blue Vital Stain Exclusion

Twenty four hours post chemotherapy drug addition, MDA-MB-231 cells already seeded in a 96-well plate are washed with 50µl Phosphate Buffered Saline (PBS) 1× then trypsinized with 10µl Trypsin (2X), and neutralized with the appropriate re-suspension media. They are then diluted with Trypan Blue on a 1:1 ratio of which 10µl is transferred to a hemacytometer counter grid for viable cell count through a light microscope. This procedure is repeated over 4 days.

F. Statistical Analysis

The statistical analysis for the FITC-dextran uptake assessments was done using t-test while for assessing caveolin-dependent endocytosis, one way Anova was used. A p-value of 0.05 represents the statistical significance. Furthermore, the average of each group, the standard deviation and the standard error of the mean were calculated and a comparison of each group to their control group was done.

CHAPTER III

RESULTS

A. Optimization of the different techniques used.

1. Optimization of HIFU parameters in the commercial HIFU transducer setup to ensure adequate mechanical sub-lethal exposure.

Numerous experimental trials were performed to optimize the HIFU parameters since we utilized a commercial HIFU transducer that is similar yet different to the custom built HIFU transducer used in previous studies in our laboratory. Similarly to the HIFU set up previously used in our laboratory, this HIFU reservoir is filled with degassed double distilled water warmed to 37 degrees. There is also an adjustable clamp that would enable us to localize in the cell sample not just at the focal spot, but also at sub-lethal HIFU exposures. The volume of the cell suspension in the sample tube was also set at 50µl and the cell count was chosen to be 200,000. The experimental parameters used were also the same corresponding to: Volts: 256Vpp, duty cycle: 2%, sonication time: 10msec, and total exposure time: 200msec, except for the frequency which was 500 KHz instead of 2 MHz. For the most part, we needed to find the location of the focal spot in order to find that of the sub-lethal percentages. In the case of the commercial HIFU transducer, its circumference is quite large which means the circumference of the focal point is also large; 40 mm, so the challenge was not to find the focal spot but to find the borders of the focal point range to determine where it begins and ends. By finding the borders of the focal point range, we determined the exact location of the focal spot by subtracting the extremities and dividing

them by 2. As a result, the focal point was determined to be 51 mm from the source of the transducer. Subsequently, we found the exact location of the sub-lethal percentage used by further calculations.

2. Quantitative assessment of cell viability of MDA-MB-231 cells post sub-lethal HIFU exposure.

MDA-MB-231 cells were exposed to two different HIFU exposures; focal spot (where cells are receiving 100% of the HIFU intensity, and sub-lethal HIFU exposure; 25.7%. After exposing the MDA-MB-231 cells to focal spot, sub-lethal HIFU and having mock HIFU cells as control, the samples were assessed over three consecutive days qualitatively by observing them using phase contrast microscopy, and quantitavely, by assessing cellular viability and proliferation using the trypan blue cell count method. Quantitative assessment by trypan blue revealed that there was no significant difference in cellular viability between mock control cells and cells subjected to sub-lethal HIFU at day 1 (*P-value>0.05*). However, the difference was significant at day 2 with a 29% decrease between the two and also at day 3 reflected in a 20% decrease (*P-value<0.05*). Nevertheless, the compiled results showed a high significant difference between the cells subjected to sub-lethal HIFU and the cells exposed to the focal point reflected in approximately 99% decrease in cell count across all three days with a (*P-value<0.01*). On the other hand, cells exposed to the focal point had very few cells with no notable proliferation over three days. Moreover, quantitative assessment by trypan blue showed a significant difference in cellular viability between cells subjected to HIFU at the focal point and the mock control cells reflected in approximately 99% decrease in cell count across all

three days with a (*P-value<0.01*) (Figure 10). Data represent mean ± SEM of three independent experiments (each done in duplicates).

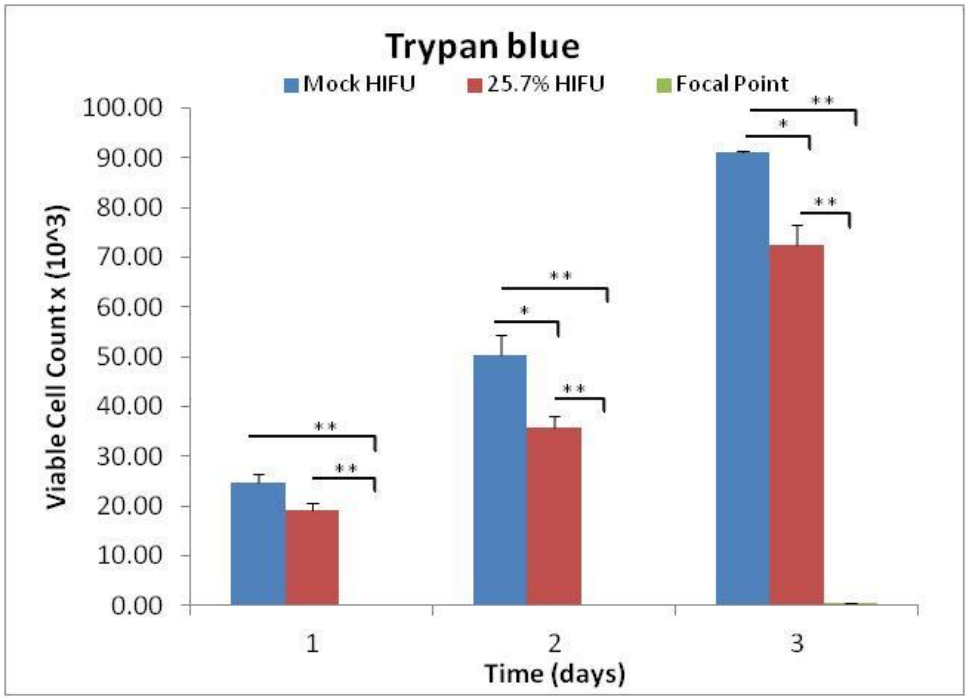

Figure 10: Quantitative assessment of cell viability & proliferation of MDA-MB-231 cells post HIFU exposure in comparison to mock – treated controls. Trypan blue viable cell counts were performed days 1-to-3 post exposure to HIFU. A significant difference in viability and proliferation was obtained between cells exposed at the focal point in comparison to the mock controls and sub-lethal HIFU exposed cells. Moreover, a significant difference was obtained between cells exposed to sub-lethal HIFU and mock HIFU cells at day 2 and day 3.Data represent mean ± SEM and asterisks represent statistical significance (*$p<0.05$; **$p<0.01$).

3. Optimization of concentration of Genistein used to inhibit caveolae-dependent endocytosis.

We aimed to test a suitable concentration of genistein that doesn't compromise cell viability of cancer cells but is also reported in the literature to inhibit caveolae-dependent endocytosis. For this purpose, several optimization experiments were performed using

various concentrations and incubation times of genistein (Data not shown). Subsequently, we chose a dose of 100μM of Genistein for an incubation time of 30 minutes as it didn't show any significance in cell viability compared to the negative control with a (*P-value>0.05*). Parallel to Genistein addition, Dimethyl sulfoxide (DMSO) was added as a vehicle to cells at a concentration of 0.1%. Likewise, no significant difference was obtained between cells treated with DMSO and cells treated with genistein and the negative control cells (*P-value>0.05*). Noteworthy, cells were treated with Genistein and DMSO 30 hours post seeding (Figure 11). Similar results were obtained for 6 hours post seeding (Data not shown). Data represent mean ± SEM of three independent experiments (each done in duplicates).

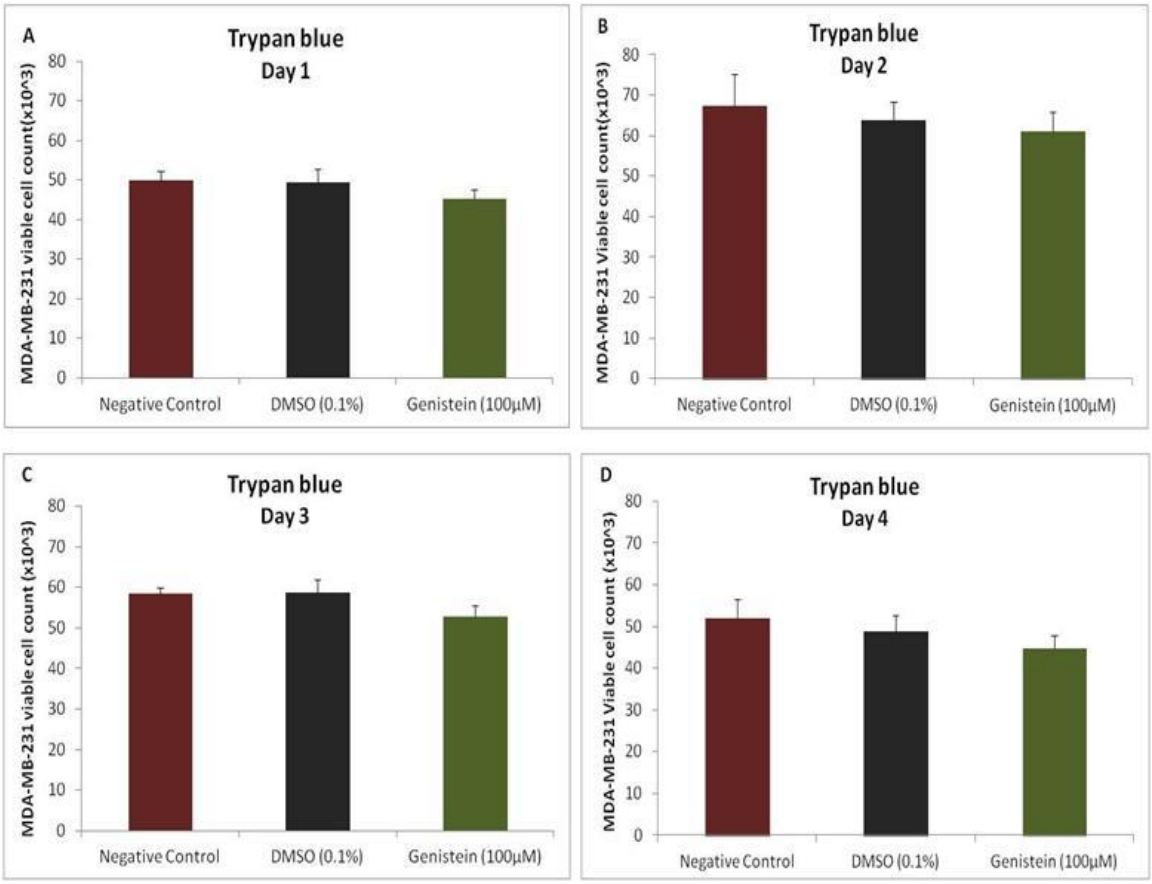

Figure 11: Assessment of viability of MDA-MB-231 cells following Genistein and DMSO treatment relative to control cells 30 hours post seeding. Trypan blue vital stain exclusion assay was used to count viable cells over a period of four days. Trypan blue assessment indicates that there is no significance difference between the negative control cells, cells treated with DMSO and cells treated with genistein. Data represent mean ± SEM of 3 independent experiments (each done in duplicates) and asterisks represent statistical significance (*$p<0.05$; **$p<0.01$).

B. Assessment of FITC-dextran uptake added to MDA-MB- 231 cells post sub-lethal HIFU exposure.

Since previous studies in our laboratory showed that sub-lethal HIFU exposure sensitizes MDA-MB-231 breast cancer cells to suboptimal cytotoxic doses of Taxol and Doxorubicin, our intention for the first aim of this study, was to determine if sonoporation is implicated as a mechanism of drug uptake. For that, MDA-MB-231 cells subjected to sub-lethal HIFU exposure and mock HIFU MDA-MB-231 cells were treated with FITC-dextran, a marker for cellular permeability, either 6 hours or 30 hours post HIFU. Assessment of FITC-dextran uptake was determined by flow cytometry and laser confocal microscopy.

1. No significant change in FITC-dextran uptake in sub-lethal HIFU exposed cells in comparison to mock – treated cells 30 hours post sub-lethal HIFU exposure by Flow Cytometry.

To assess FITC-dextran uptake in sub-lethal HIFU exposed cells vs. mock – treated MDA-MB-231 cells 30 hours post sub-lethal HIFU exposure by flow cytometry, we analyzed six test samples; negative control cells (cells not exposed to HIFU nor stained with FITC-Dextran), positive control cells (cells permeabilized with digitonin and stained with FITC-Dextran), 25.7% HIFU exposed cells stained with FITC-Dextran, 25.7% HIFU exposed cells negative for FITC-Dextran, mock HIFU cells stained with FITC, and mock HIFU cells negative for FITC-Dextran. Flow cytometry data analysis revealed that the percentage of positive cells for FITC-Dextran in mock HIFU cells is 36% in comparison to that of the sub-lethal HIFU cells which is 38%. However, this slight increase, was not shown to be statistically significant between them with a (*P-value>0.05*). Moreover, a

significant difference in percentage of positive cells for FITC-Dextran have been observed between mock HIFU cells stained with FITC-Dextran and its respected control; mock HIFU cells negative for FITC-Dextran with a (*P-value<0.01*). In other words, percentage of positive cells in mock HIFU cells negative for FITC-Dextran is 2.2% which is 34% lower than that of mock HIFU cells stained with FITC-Dextran. Likewise, a significant difference in percentage of positive cells for FITC-Dextran have been observed between sub-lethal HIFU cells stained with FITC-Dextran and its respected control; sub-lethal HIFU cells negative for FITC-Dextran reflected in a 32% decrease with a (*P-value<0.01*). Additionally, quantification by flow cytometry has shown that percentage of positive cells for FITC-Dextran is 50% in positive controls and 3% in negative controls (Figure 12B). Data represent mean ± SEM of four independent experiments.

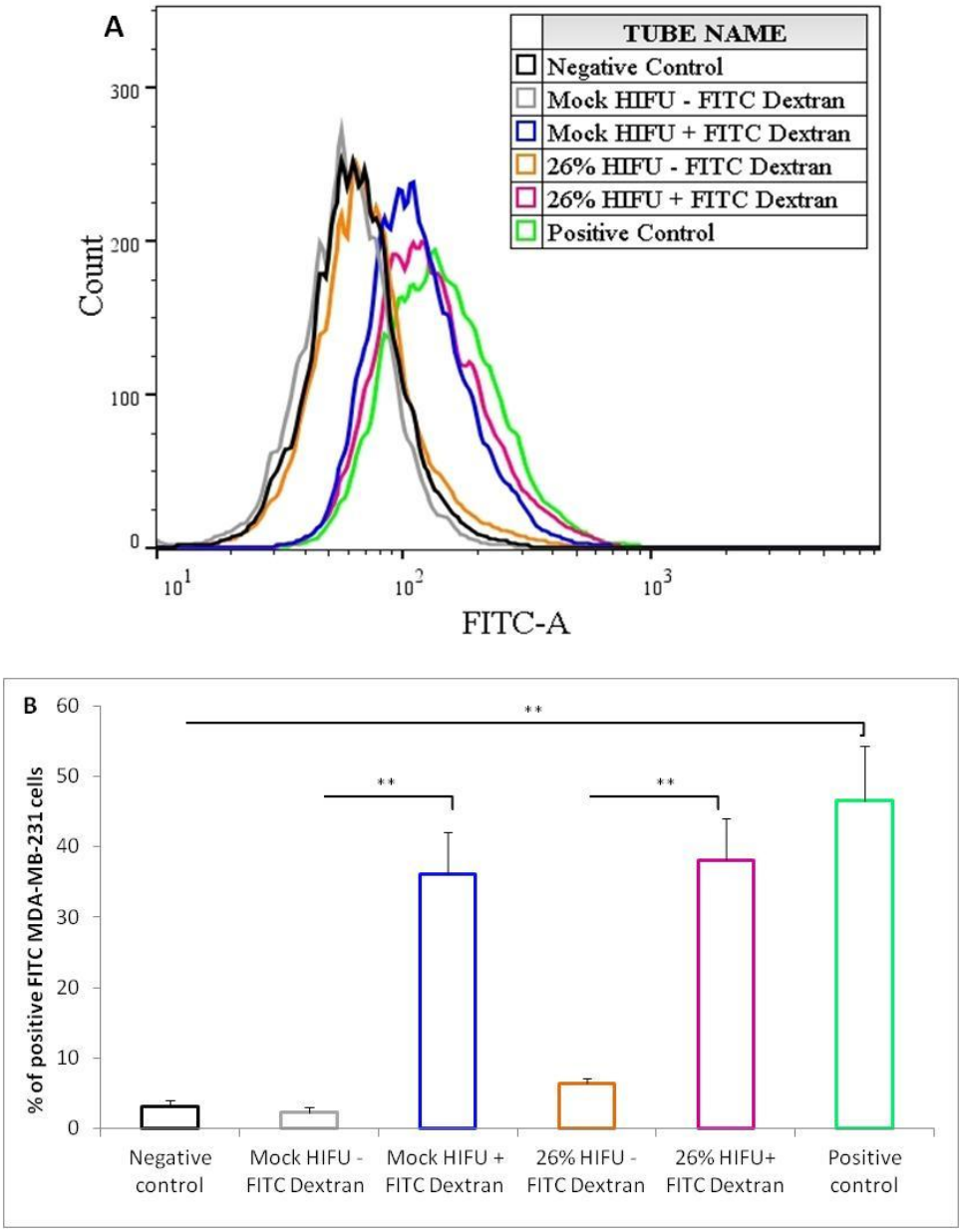

Figure 12: Flow cytometry representative (A) and quantification of positive MDA-MB-231 cells (B) for FITC-dextran in negative control cells, positive control cells, mock-treated cells stained with FITC-dextran, mock HIFU cells negative for FITC-dextran, sub-lethal HIFU cells stained with FITC-dextran and sub-lethal HIFU cells negative for FITC-dextran 30hr post HIFU exposure. No significant difference is observed between cells exposed to sub-lethal HIFU cells and mock controls. Illustration is a representative of 3 independent repeats. Data represent mean ± SEM of four independent experiments,

2. No significant change in FITC-dextran uptake in sub-lethal HIFU exposed cells in comparison to mock – treated cells 30 hours post sub-lethal HIFU exposure by Laser Confocal Microscopy.

In order to further validate the uptake of FITC-dextran at 30hr in sub-lethal HIFU exposed cells vs. mock control cells determined by flow cytometry, we followed the same procedure but stained the cells on coverslips instead and mounted them on slides to observe and acquire 2-D fluorescent images using laser confocal microscopy. Using the same exposure time and excitation wavelength, we obtained eight image frames for the sub-lethal HIFU exposed MDA-MB-231 cells and mock HIFU MDA-MB-231 cells. Qualitative analysis and cytoplasmic scoring was performed visually, by observing and comparing the FITC-dextran stain for each test sample (Figure 13A). On average, around 700 cells from each test were assessed. The data indicates an increase by 4% in FITC-dextran uptake in HIFU exposed cells in comparison to the mock HIFU cells. This increase, however, was not determined to be statistically significant (*P-value >0.05*). Cells permeabilized with digitonin and stained with FITC-dextran were used as a positive control. Likewise, using the same exposure time and excitation wavelength, we obtained four image frames. On average, 300 cells were assessed. As a result, data reveals a significant difference between Mock HIFU cells and HIFU exposed cells in comparison to the positive control (*P-value<0.05*) (Figure 13B). Scoring analysis data is represented as mean ± SEM of three independent experiments.

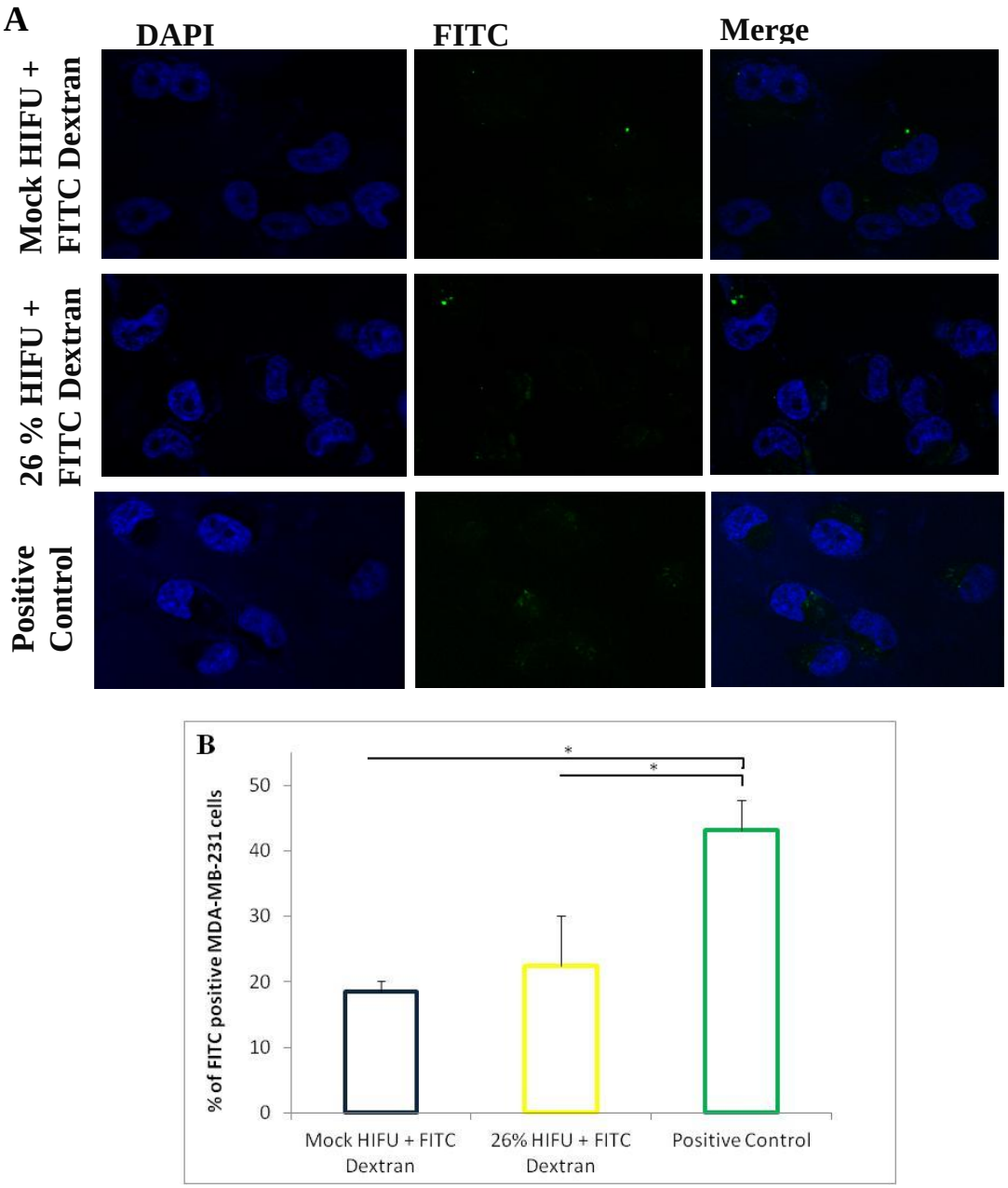

Figure 13: Visual cytoplasmic scoring of FITC-dextran uptake in sub-lethal HIFU exposed MDA-MB-231 cells vs. mock control cells 30 hours post HIFU exposure. Top Panel (A) are representative laser confocal microscopy images acquired at 63x magnification. DAPI was used to stain the nuclei (uppermost panel). FITC-dextran stain is shown in green (middle panel). Lower Panel (B) shows data obtained from cytoplasmic scoring. Visual scoring reveals no significant change in the uptake of FITC-dextran 30 hours post sub-lethal HIFU exposure in comparison to mock controls. Mock controls and HIFU exposed cells were shown to be significantly different from that of the positive control used. Data represent mean ± SEM of three independent experiments within an average of 700 cells scored for mock HIFU cells and also for HIFU exposed cells and an average of 300 cells for positive control cells.

3. No significant change in FITC-dextran uptake in sub-lethal HIFU exposed cells in comparison to mock – treated cells 6 hours post sub-lethal HIFU exposure by Laser Confocal Microscopy.

We also wanted to assess the uptake of FITC-Dextran in sub-lethal HIFU exposed cells in comparison to mock HIFU cells 6 hours post sub-lethal HIFU exposure by laser confocal microscopy. Similarly to the 30hr time point, we obtained eight image frames for HIFU exposed MDA-MB-231 cells and mock HIFU MDA-MB-231 cells using the same exposure time and excitation wavelength. Qualitative analysis and cytoplasmic scoring was performed visually, by observing and comparing the FITC-dextran stain for each test sample (Figure 14A). On average, around 700 cells from each test were assessed. The data indicates an increase by 2% in HIFU exposed cells in comparison to the mock HIFU cells. This increase, however, was not determined to be significant (*P-value >0.05*). As for the positive control, we obtained four image frames using the same exposure time and excitation wavelength. On average, 300 cells were assessed. As a result, data reveals a significant difference between Mock HIFU cells and HIFU exposed cells in comparison to the positive control (*P-value<0.05*) (Figure 14B). Scoring analysis data is represented as mean ± SEM of three independent experiments.

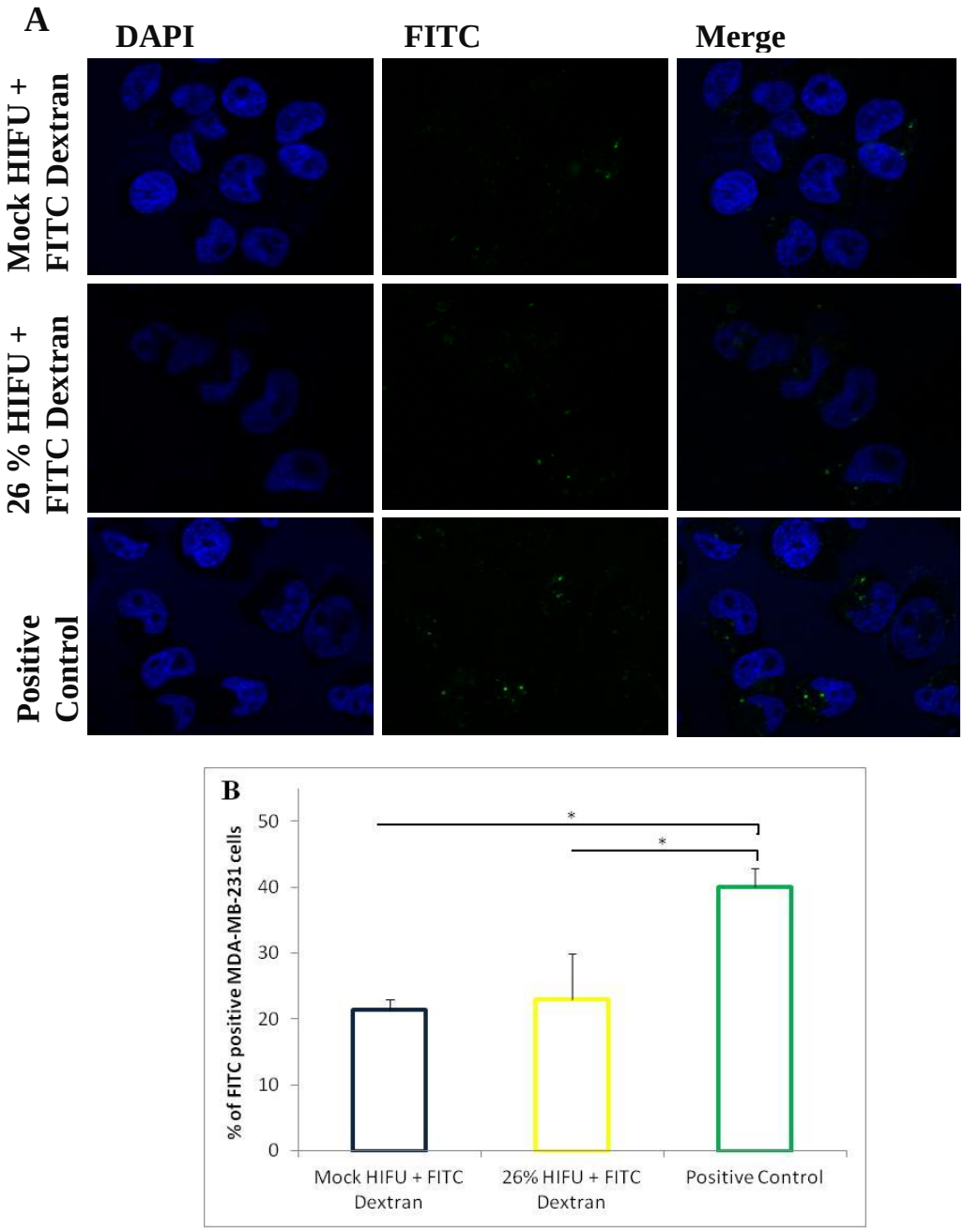

Figure 14: Visual cytoplasmic scoring of FITC-dextran uptake in sub-lethal HIFU exposed MDA-MB-231 cells vs. mock-treated control cells 6 hours post HIFU exposure. Top Panel (A) are representative laser confocal microscopy images acquired at 63x magnification. DAPI was used to stain the nuclei (uppermost panel). FITC-dextran stain is shown in green (middle panel). Lower Panel (B) shows data obtained by cytoplasmic scoring. Visual scoring reveals no significant change in the uptake of FITC-dextran 6 hours post sub-lethal HIFU exposure in comparison to mock HIFU. Mock control cells and HIFU exposed cells were shown to be significantly different from that of the positive control used. Data represent mean ± SEM of three independent experiments within an average of 700 cells scored for mock HIFU cells and for HIFU exposed cells and an average of 300 cells for positive control cells.

C. Pre-treatment with Genistein reverses the enhanced *in vitro* sensitivity of MDA-MB-231 cells to sub-cytotoxic concentrations of Taxol and Doxil post-sub-lethal HIFU exposure.

For the second aim of this study, we wanted to determine if caveolae-dependent endocytosis is implicated as a mechanism of drug uptake in the enhanced *in vitro* sensitivity of MDA-MB-231 cells to sub-lethal anti-neoplastic agent's concentration post-sub-lethal HIFU exposure. For that, MDA-MB-231 cells subjected to sub-lethal HIFU exposure and mock HIFU were pre-treated with Genistein, a specific potent inhibitor of the caveolae-dependent endocytosis pathway, either 6 hours or 30 hours post HIFU. Subsequently, cells were exposed to either Taxol or Doxorubicin and cellular viability was quantified using trypan blue vital stain exclusion assay over four days. Percentage of viable MDA-MB-231 cells across all tested samples was determined and plotted in respect to the ultimate Mock HIFU control cells (untreated with anti-neoplastic agents and genistein) which were designated as 100% viable across each day.

1. Quantitative assessment of Genistein and Taxol added to MDA-MB- 231 cells 6 hours post sub-lethal HIFU exposure.

To determine if pre-treatment with genistein 6 hours post sub-lethal HIFU exposure will revert the enhanced *in vitro* sensitivity of MDA-MB-231 cells to the two sub-lethal concentrations of Taxol, trypan blue vital stain exclusion assay was performed on MDA-MB-231 cells post sub-lethal HIFU exposure, genistein and taxol addition over a period of four days. At Day 1, for cells treated with 0 nM of Taxol, trypan blue assessment showed no significant difference in cellular viability between the mock HIFU cells treated with genistein and the mock HIFU cells untreated with genistein. Similarly, no significant

difference in cellular viability was noted between the sub-lethal HIFU cells treated with genistein and sub-lethal HIFU cells untreated with genistein (*P-value>0.05*). Nevertheless, trypan blue assessment revealed that cellular viability in sub-lethal HIFU cells untreated with genistein was decreased by 32% when compared to the mock HIFU cells untreated with genistein and this difference was shown to be statistically significant with a (*P-value<0.01*). Moreover, a significant difference was noted between the mock HIFU cells untreated with genistein and sub-lethal HIFU cells treated with genistein reflected in a 45% decrease in cellular viability with a (*P-value<0.01*). Likewise, similar results were obtained between sub-lethal HIFU cells treated and untreated with genistein when compared to mock HIFU cells treated with genistein. Similarly to cells treated with 0 nM of taxol, a similar pattern was obtained for cells treated with 1.5 nM of Taxol. Cellular viability of sub-lethal HIFU cells treated and untreated with Genistein was significantly reduced by 21% in both panels when compared to mock HIFU cells treated and untreated with Genistein (*P-value<0.05*). As for cells treated with 7.5 nM of Taxol, cellular viability of sub-lethal HIFU cells untreated with genistein was shown to be significantly lower by 24% in comparison to mock HIFU cells treated with Genistein (*P-value<0.05*). Noteworthy, cellular viability was increased by 8% in mock HIFU cells treated with Genistein when compared to mock HIFU cells untreated with Genistein. Likewise, cellular viability was increased by 14% in sub-lethal HIFU cells treated with genistein when compared to sub-lethal HIFU cells untreated with Genistein. This increase, however, was not statistically significant from that of the cells untreated with Genistein (*P-value>0.05*). Additionally, percentage of cellular viability of mock HIFU cells treated with 7.5 nM of Taxol and mock HIFU cells treated with 1.5 nM were significantly reduced by 69% and

45% correspondingly when compared to mock HIFU cells untreated with Taxol with a (*P-value<0.01*). Likewise, percentage of cellular viability of sub-lethal HIFU cells treated with 7.5 nM of Taxol and sub-lethal HIFU cells treated with 1.5 nM were significantly reduced by 34% and 53% correspondingly when compared to sub-lethal HIFU cells untreated with taxol with a (*P-value<0.01*). Data represent mean percentage difference ± SEM of three independent experiments, each done in duplicates (Figure 15A, see below).

At Day 2, for cells treated with 0 nM of Taxol, similar results were obtained to that of cells treated with 0 nM of Taxol at day 1. As for cells treated with 1.5 nM of Taxol, cellular viability was significantly reduced by 12% in sub-lethal HIFU cells untreated with Genistein when compared to mock HIFU cells untreated with Genistein with a (*P-value<0.01*). Moreover, percentage of cellular viability was significantly reduced by 9% in sub-lethal HIFU cells treated with Genistein when compared to mock HIFU cells untreated with Genistein (*P-value<0.05*). Cellular viability was also significantly reduced by 10% in sub-lethal HIFU cells untreated with Genistein when compared to mock HIFU cells treated with Genistein with a (*P-value<0.05*). MDA-MB-231 cells exposed to sub-lethal HIFU and treated with Genistein revealed a 3% increase in cellular viability in comparison to cells exposed to sub-lethal HIFU but untreated with Genistein. This increase, however, was not determined to be statistically significant (*P-value>0.05*). As for cells treated with 7.5 nM of Taxol, cellular viability was significantly reduced by 6% in sub-lethal HIFU cells untreated with genistein when compared to mock HIFU cells untreated with Genistein and mock HIFU cells treated with Genistein. Moreover, a slight increase by 2% in cellular viability was observed in cells exposed to sub-lethal HIFU and treated with Genistein when compared to cells exposed to sub-lethal HIFU and untreated with Genistein. This slight

increase, however, was not determined to be statistically significant (*P-value>0.05*). Additionally, percentage of cellular viability of mock HIFU cells treated with 7.5 nM of Taxol and mock HIFU cells treated with 1.5 nM were significantly reduced by 88% and 75% correspondingly when compared to mock HIFU cells untreated with Taxol with a (*P-value<0.01*). Likewise, percentage of cellular viability of sub-lethal HIFU cells treated with 7.5 nM of Taxol and sub-lethal HIFU cells treated with 1.5 nM were significantly reduced by 94% and 87% correspondingly when compared to sub-lethal HIFU cells untreated with taxol with a (*P-value<0.01*). Data represent mean percentage difference ± SEM of three independent experiments, each done in duplicates (Figure 15B, see below)

At day 3, for cells treated with 0 nM of Taxol, cellular viability was nearly 30% significantly reduced in cells exposed to sub-lethal HIFU and untreated with Genistein in comparison to mock HIFU cells untreated with genistein with a (*P-value<0.05*). Additionally, cellular viability was significantly reduced by 35% in cells exposed to sub-lethal HIFU and untreated with genistein in comparison to mock HIFU cells untreated with genistein and mock HIFU cells treated with Genistein with a (*P-value<0.05*). As for cells treated with 1.5 nM of Taxol, cellular viability was increased by 7% in mock HIFU cells treated with Genistein when compared to mock HIFU cells untreated with Genistein. This increase was statistically significant with a (*P-value<0.01*). A significant reduction by 6% was noted in cells exposed to sub-lethal HIFU and untreated with genistein when compared to mock HIFU cells untreated with Genistein with a (*P-value<0.01*). Moreover, cellular viability was significantly reduced by 13% in cells exposed to sub-lethal HIFU and untreated with Genistein when compared to mock HIFU cells treated with Genistein with a (*P-value<0.05*). Moreover, a 10% significant decrease in cellular viability was noted in

cells exposed to sub-lethal HIFU and treated with genistein when compared to mock HIFU cells treated with genistein with a (*P-value<0.05*). A 3% increase was noted in cells exposed to sub-lethal HIFU and treated with Genistein relative to the cells exposed to sub-lethal HIFU and untreated with Genistein, yet it was not determined to be statistically significant with a (*P-value>0.05*). As for cells treated with 7.5 nM of Taxol, cellular viability was significantly reduced by 3% in cells exposed to sub-lethal HIFU and untreated with Genistein when compared to mock HIFU cells untreated with Genistein with a (*P-value<0.05*) and by 5% when compared to mock HIFU cells treated with Genistein with a (*P-value<0.01*). Moreover, a 3% decrease in cellular viability in sub-lethal HIFU cells treated with Genistein was observed when compared to mock HIFU cells treated with Genistein with a (*P-value<0.05*). Noteworthy, a 2% increase was observed in mock HIFU cells treated with Genistein and sub-lethal HIFU cells treated with Genistein when compared to mock HIFU untreated with Genistein and sub-lethal untreated with Genistein respectively. This increase, however, was shown not to be statistically significant (*P-value>0.05*). Additionally, percentage of cellular viability of mock HIFU cells treated with 7.5 nM of Taxol and mock HIFU cells treated with 1.5 nM were significantly reduced by 94% and 88% correspondingly when compared to mock HIFU cells untreated with Taxol with a (*P-value<0.01*). Likewise, percentage of cellular viability of sub-lethal HIFU cells treated with 7.5 nM of Taxol and mock HIFU cells treated with 1.5 nM were significantly reduced by 68% and 65% correspondingly when compared to sub-lethal HIFU cells untreated with Taxol. Data represent mean percentage difference ± SEM of three independent experiments, each done in duplicates (Figure 15C, see below).

At day 4, for cells treated with 0 nM of Taxol addition, a similar pattern was obtained as for cells treated with 0 nM of Taxol at day 1. Concerning the cells treated with 1.5 nM Taxol, around 2-3 % increase in cellular viability was observed in mock HIFU cells treated with Genistein and sub-lethal HIFU cells treated with Genistein in comparison to mock control cells untreated with Genistein and sub-lethal HIFU untreated with Genistein respectively. This increase, however, was not determined to be statistically significant (*P-value>0.05*). Additionally, percentage of cellular viability of mock HIFU cells treated with 7.5 nM of Taxol and mock HIFU cells treated with 1.5 nM were significantly reduced by 98% and 93% correspondingly when compared to mock HIFU cells untreated with Taxol with a (*P-value<0.01*). Likewise, percentage of cellular viability of sub-lethal HIFU cells treated with 7.5 nM of Taxol and mock HIFU cells treated with 1.5 nM were significantly reduced by 80% and 77% correspondingly when compared to sub-lethal HIFU cells untreated with Taxol with a (*P-value<0.01*). Data represent mean percentage difference ± SEM of three independent experiments, each done in duplicates (Figure 15D, see below).

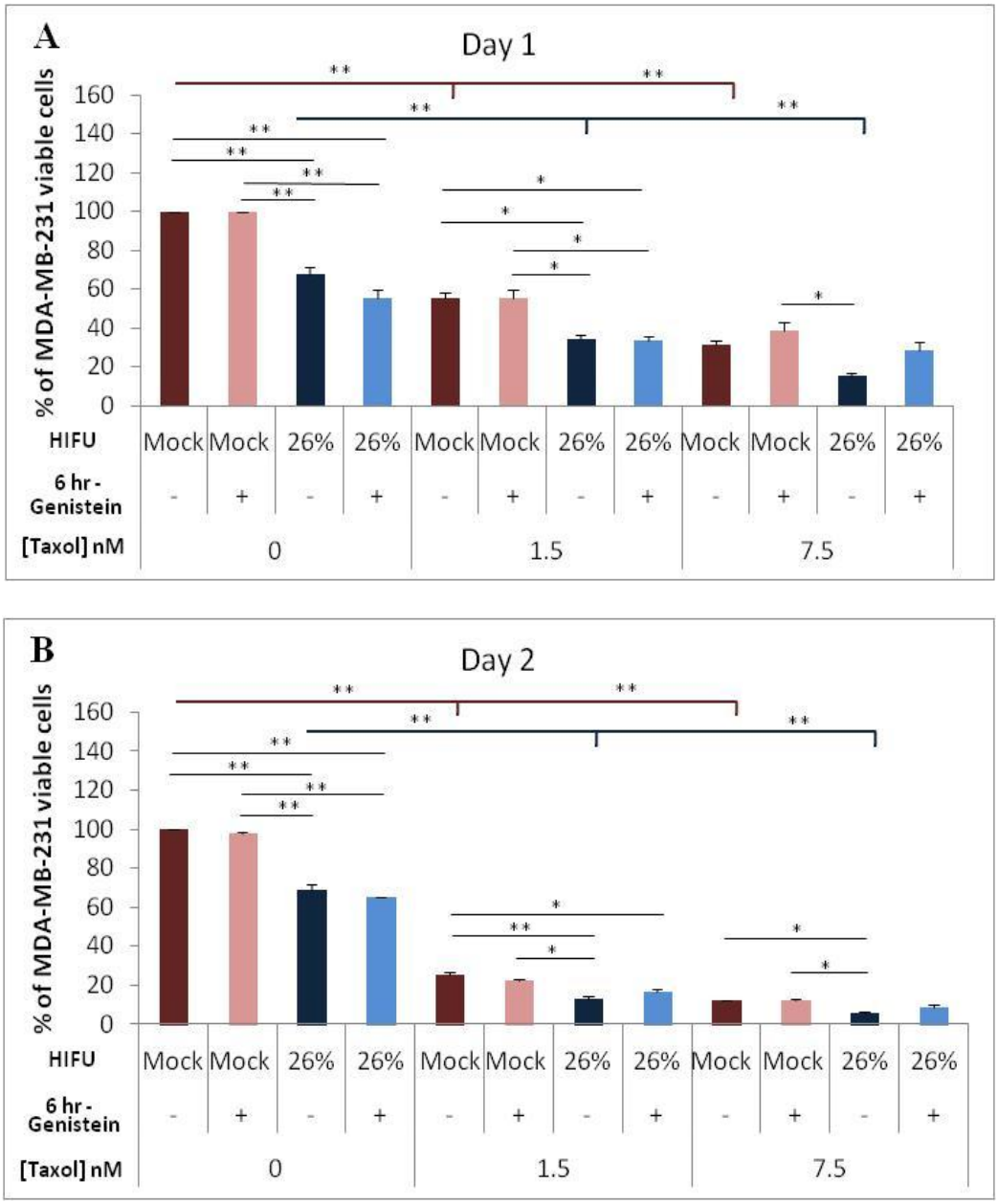

Figure 15: MDA-MB-231 cell viability following Taxol and Genistein pretreatment at 6hr post sub-lethal HIFU exposure (26%). Trypan blue vital stain exclusion assay was used to count viable cells over a period of four days. Trypan blue assessment suggests that there is an enhanced *in vitro* sensitivity of MDA-MB-231 cells to sub-cytotoxic doses of Taxol post sub-lethal HIFU and this sensitivity is reverted by the addition of genistein. Moreover, it was significant between mock HIFU cells treated and untreated with genistein at day 3. Data represent mean percentage ± SEM of 3 independent experiments (each done in duplicates; * *p<0.05; **p<0.01*).

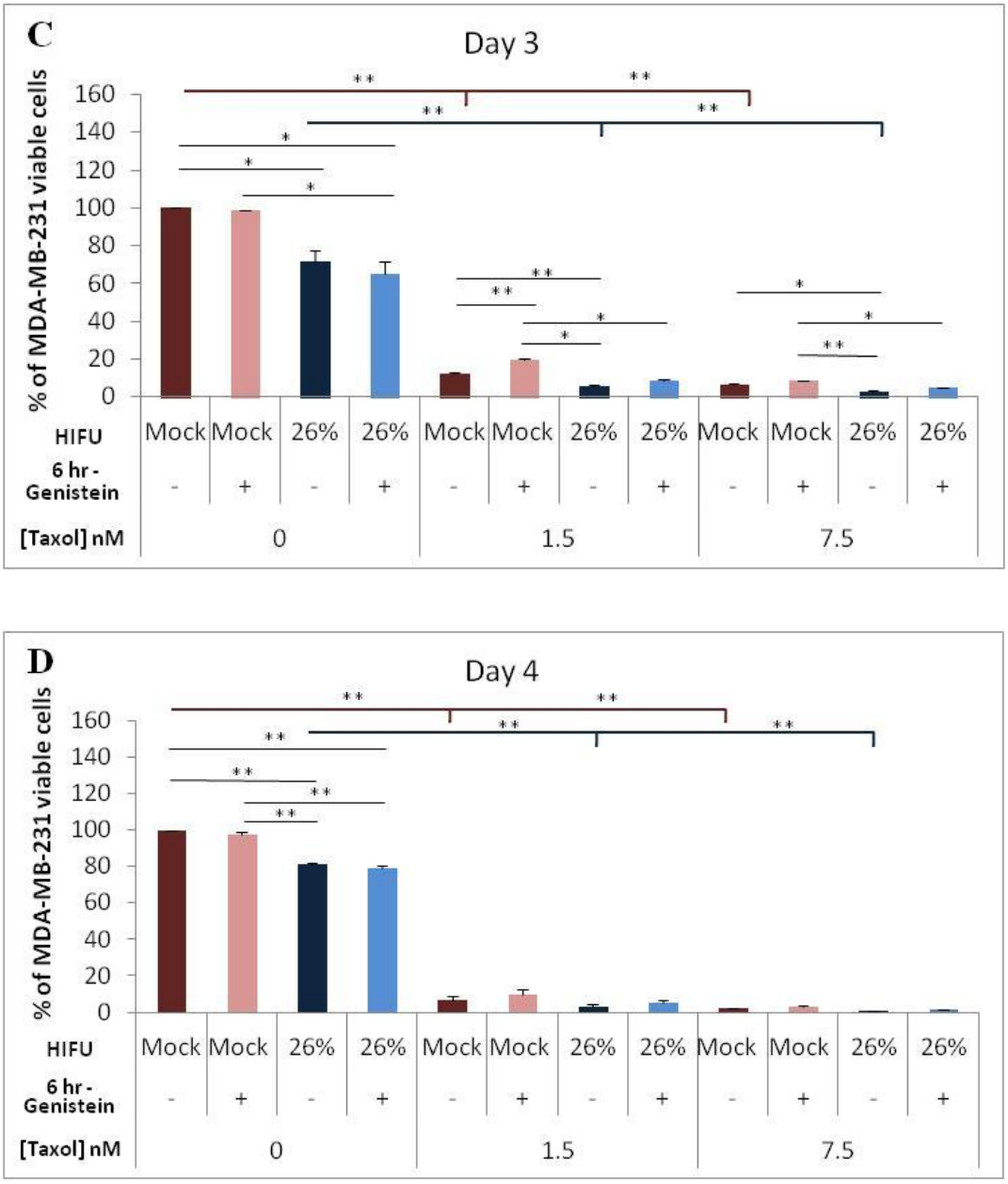

Figure 15: MDA-MB-231 cell viability following Taxol and Genistein pretreatment at 6hr post sub-lethal HIFU exposure (26%). Trypan blue vital stain exclusion assay was used to count viable cells over a period of four days. Trypan blue assessment suggests that there is an enhanced *in vitro* sensitivity of MDA-MB-231 cells to sub-cytotoxic doses of Taxol post sub-lethal HIFU and this sensitivity is reverted by the addition of Genistein. Moreover, it was significant between mock HIFU cells treated and untreated with Genistein at day 3. Data represent mean percentage ± SEM of 3 independent experiments (each done in duplicates; * *p<0.05; **p<0.01*).

2. Quantitative assessment of Genistein and Taxol added to MDA-MB- 231 cells 30 hours post sub-lethal HIFU exposure.

Similarly to the assessment of Genistein and Taxol added on MDA-MB-231 cells 6 hours post sub-lethal HIFU exposure, we wanted to assess it 30 hours post sub-lethal HIFU exposure. At Day 1, for cells treated with 0 nM of Taxol, trypan blue assessment showed no significant difference in cellular viability between the mock HIFU cells treated with Genistein and the mock HIFU cells untreated with genistein. Similarly, no significant difference in cellular viability was noted between the cells subjected to sub-lethal HIFU treated with Genistein and cells subjected to sub-lethal HIFU and untreated with Genistein with a (*P-value>0.05*). A 28% reduction was noted in cells exposed to sub-lethal HIFU and treated with Genistein when compared to mock HIFU cells untreated with Genistein and this reduction was shown to be statistically significant with a (*P-value<0.05*). As for cells treated with 1.5 nM Taxol, it is worth mentioning that there is a 10% increase in cellular viability in mock HIFU cells treated with genistein in comparison to mock HIFU cells untreated with Genistein. Similarly, there is a 3% increase in cellular viability in cells subjected to sub-lethal HIFU and treated with genistein in comparison to cells subjected to sub-lethal HIFU but untreated with Genistein. The increase, however, was not determined to be statistically significant (*P-value>0.05*). Likewise, for cells treated with 7.5 nM of Taxol, a 2% increase in cellular viability was noted in mock HIFU cells treated with genistein in comparison to mock control cells untreated with Genistein. In the same way, a 5% increase in cellular viability was observed in cells subjected to sub-lethal HIFU and treated with Genistein in comparison to cells subjected to sub-lethal HIFU and untreated with Genistein, yet this was also determined not to be statistically significant (*P-*

value>0.05). Data represent mean percentage difference ± SEM of three independent experiments, each done in duplicates. (Figure 16A, see below).

At day 2, for cells treated with 0 nM of Taxol, 1.5 nM of Taxol and 7.5 nM of Taxol, trypan blue assessment revealed a similar pattern to the cells treated with 0 nM of Taxol, 1.5 nM of Taxol and 7.5 nM of Taxol, at day 2 post 6hr of sub-lethal HIFU exposure. Data represent mean percentage difference ± SEM of three independent experiments, each done in duplicates. (Figure 16B, see below).

At day 3, for cells treated with 0, 1.5, and 7.5 nM of Taxol, a similar pattern was obtained to that of cells treated with 0, 1.5, and 7.5 nM of Taxol, at day 3 6hr post sub-lethal HIFU exposure. Data represent mean percentage difference ± SEM of three independent experiments, each done in duplicates (Figure 16C, see below).

Likewise, at day 4, for cells treated with 0 nM, 1.5 nM, and 7.5 nM of Taxol, a similar pattern was obtained to that of cells treated with 0 nM of taxol, 1.5 nM of taxol and 7.5 nM of Taxol, at day 4 6hr post sub-lethal HIFU exposure. Data represent mean percentage difference ± SEM of three independent experiments, each done in duplicates (Figure 16D, see below).

Across all days, percentage of cellular viability of mock HIFU cells treated with 7.5 nM of Taxol and mock HIFU cells treated with 1.5 nM were significantly reduced in comparison to mock HIFU cells untreated with taxol with a (*P-value<0.01*). Likewise, percentage of cellular viability of sub-lethal HIFU cells treated with 7.5 nM of Taxol and

mock –HIFU cells treated with 1.5 nM were significantly reduced in comparison to sub-lethal HIFU cells untreated with Taxol with a (*P-value<0.01*).

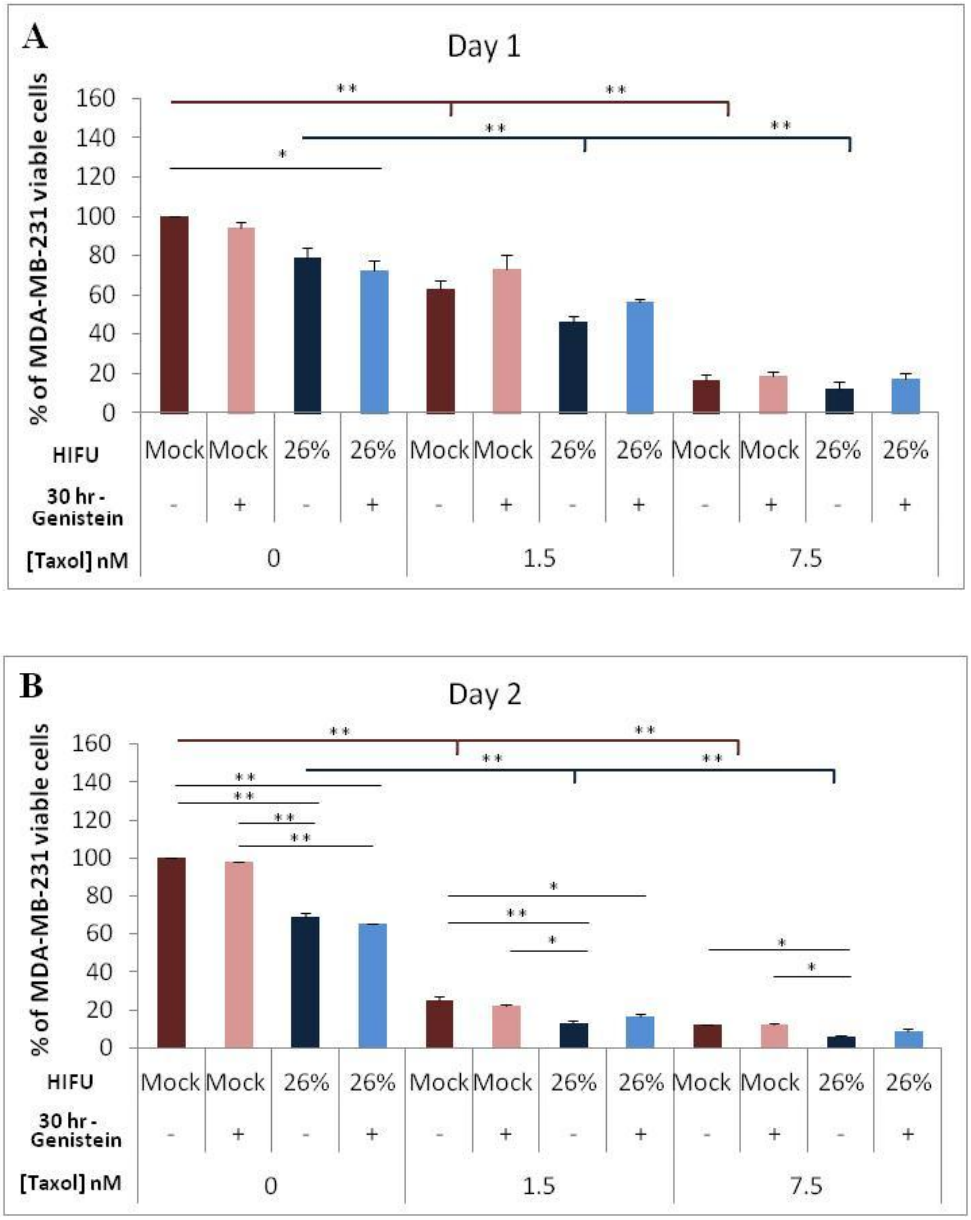

Figure 16: MDA-MB-231 cell viability following Taxol and Genistein pretreatment at 30hr post sub-lethal HIFU exposure (26%). Trypan blue vital stain exclusion assay was used to count viable cells over a period of four days. Trypan blue assessment suggests that there is an enhanced *in vitro* sensitivity of MDA-MB-231 cells to sub-cytotoxic doses of Taxol post sub-lethal HIFU and this sensitivity is reverted by the addition of Genistein, yet it was not determined to be statistically significant. Data represent mean percentage ± SEM of 3 independent experiments (each done in duplicates; * *p<0.05; **p<0.01*).

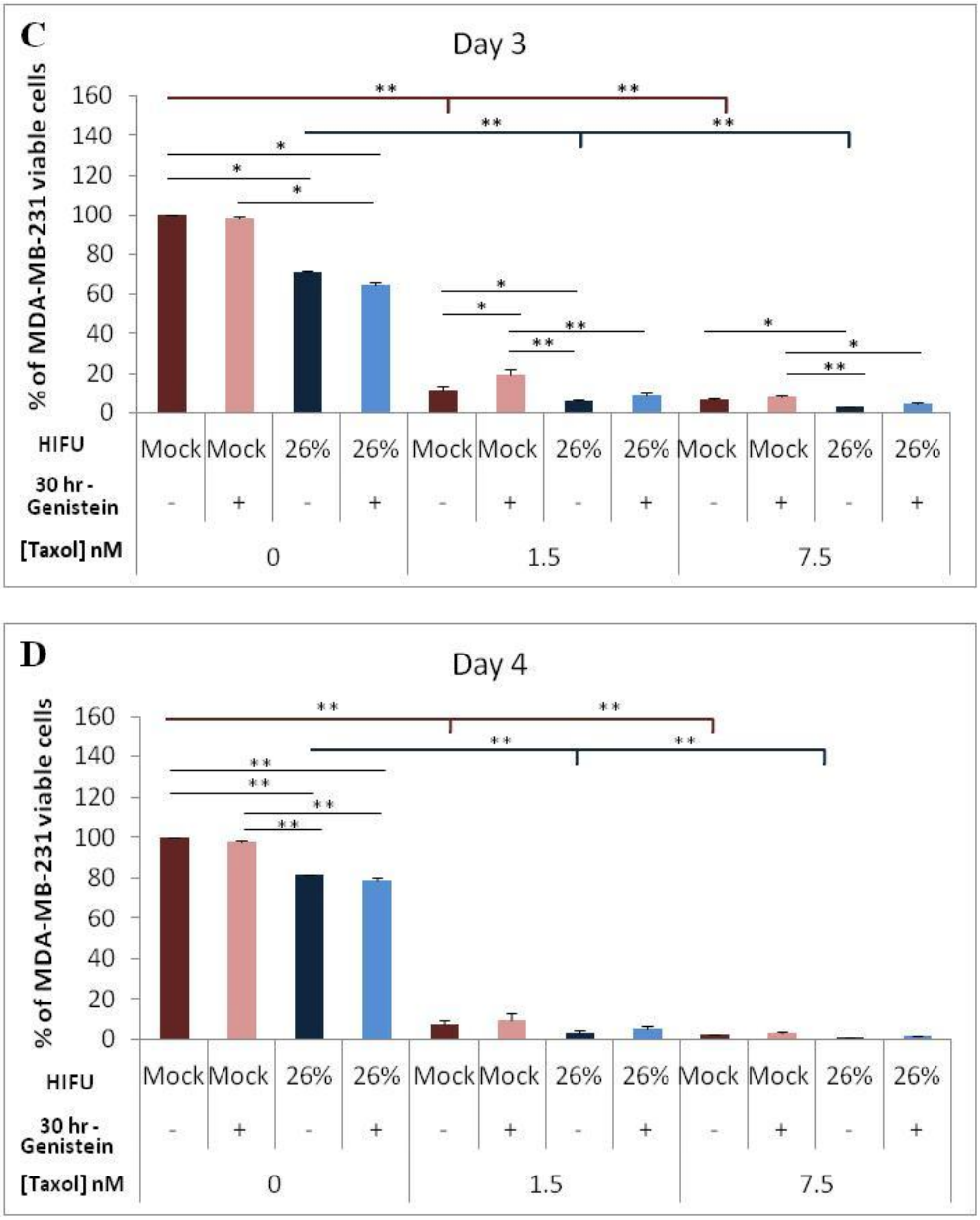

Figure 16: MDA-MB-231 cell viability following Taxol and Genistein pretreatment at 30hr post sub-lethal HIFU exposure (26%). Trypan blue vital stain exclusion assay was used to count viable cells over a period of four days. Trypan blue assessment suggests that there is an enhanced *in vitro* sensitivity of MDA-MB-231 cells to sub-cytotoxic doses of Taxol post sub-lethal HIFU and this sensitivity is reverted by the addition of Genistein, yet it was not determined to be statistically significant. Data represent mean percentage ± SEM of 3 independent experiments (each done in duplicates; ** $p<0.05$; **$p<0.01$*).

3. Quantitative assessment of Genistein and Doxil added to MDA-MB- 231 cells 6 hours post sub-lethal HIFU exposure.

Cellular viability of MDA-MB-231 cells was also assessed after the addition of Genistein and Doxil 6 hours post sub-lethal HIFU exposure by trypan blue exclusion assay over a period of four days. At day 1, for cells treated with 0 µM of doxorubicin, trypan blue assessment indicated a similar pattern to that of cells treated with 0 nM of Taxol at day 1 6 hours post sub-lethal HIFU exposure. As for cells treated with 0.05 µM of doxorubicin, a 4% increase in cellular viability was obtained in mock HIFU cells treated with Genistein compared to mock HIFU cells untreated with Genistein. This increase, however, was not determined to be statistically significant (*P-value>0.05*). Similarly, in cells treated with 0.5 µM of doxorubicin, an 11% increase in cellular viability was obtained in cells subjected to mock HIFU cells and treated with Genistein when compared to mock HIFU cells untreated with Genistein. Nevertheless, we did not detect any significant difference between them (*P-value>0.05*). Moreover, a 6% increase was determined in cells exposed to sub-lethal HIFU and treated with Genistein in comparison to cells exposed to sub-lethal HIFU and untreated with Genistein, yet no significant difference was obtained (*P-value>0.05).* Moreover, a 32% significant reduction was obtained in cells exposed to sub-lethal HIFU and untreated with Genistein when compared to mock HIFU cells treated with Genistein with a (*P-value<0.05*). Data represent mean percentage difference ± SEM of three independent experiments, each done in duplicates (Figure 17A, see below).

At day 2, for cells treated with 0 µM of doxorubicin, trypan blue assessment indicated a similar pattern to that of cells treated with 0 nM of Taxol at day 1 6 hours post

sub-lethal HIFU exposure. As for cells treated with 0.05 µM of doxorubicin, a 2% increase in cellular viability was obtained in mock HIFU cells and sub-lethal HIFU cells treated with Genistein when compared to mock control cells and sub-lethal cells untreated with Genistein. This increase, however, was shown not to be statistically significant (*P-value>0.05*). Likewise, for cells treated with 0.5 µM of doxorubicin, a 3% increase in cellular viability was obtained in mock HIFU cells and sub-lethal HIFU cells treated with Genistein when compared to mock HIFU cells and sub-lethal cells untreated with Genistein, yet this was shown not to be statistically significant (*P-value>0.05*). Data represent mean percentage difference ± SEM of three independent experiments, each done in duplicates (Figure 17B, see below).

At day 3, for cells treated with 0 µM of doxorubicin, a similar pattern of results was obtained to that of cells treated with 0 nM of Taxol at day 1 6 hours post sub-lethal HIFU exposure. As for cells treated with 1.5 nM, a slight increase of 1% in cellular viability was indicated in mock HIFU cells treated with genistein in comparison to mock HIFU cells untreated with Genistein. Moreover, a slight increase of 2% in cellular viability was determined in cells exposed to sub-lethal HIFU and treated with Genistein in comparison to cells exposed to sub-lethal and untreated with Genistein. Nevertheless, this was not determined to be statistically significant (*P-value>0.05*). Data represent mean percentage difference ± SEM of three independent experiments, each done in duplicates (Figure 17C, see below).

At day 4, for cells treated with 0 µM of doxorubicin, cellular viability was reduced by 20% in cells exposed to sub-lethal HIFU and untreated with genistein and by 22% in

sub-lethal HIFU cells and treated with Genistein in comparison mock HIFU cells untreated with Genistein. Both reductions were shown to be statistically significant with a (*P-value<0.05*). As for cells treated with 0.05 µM of doxorubicin, cellular viability was reverted by 7% in mock control cells treated with Genistein and by 5% in sub-lethal HIFU cells treated with Genistein in comparison to mock HIFU cells untreated with Genistein and sub-lethal HIFU cells untreated with Genistein respectively. However, this was not determined to be statistically significant (*P-value>0.05*). As for cells treated with 0.5µM of doxorubicin, a 2% increase in cellular viability was obtained in mock HIFU cells and sub-lethal cells treated with Genistein in comparison to mock HIFU cells and sub-lethal cells untreated with Genistein. However, this increase was not shown to be significant with a (*P-value>0.05).* Data represent mean percentage difference ± SEM of three independent experiments, each done in duplicates (Figure 17D, see below).

Across all days, percentage of cellular viability of mock HIFU cells treated with 0.5µM of doxorubicin and mock control cells treated with 0.05 µM of doxorubicin were significantly reduced in comparison to mock HIFU cells treated with 0 µM of doxorubicin (*P-value<0.01*). Likewise, percentage of cellular viability of sub-lethal HIFU cells treated with 0.5µM of doxorubicin and mock HIFU cells treated with 0.05 µM of doxorubicin were significantly reduced in comparison to mock HIFU cells treated with 0 µM of doxorubicin (*P-value<0.01*).

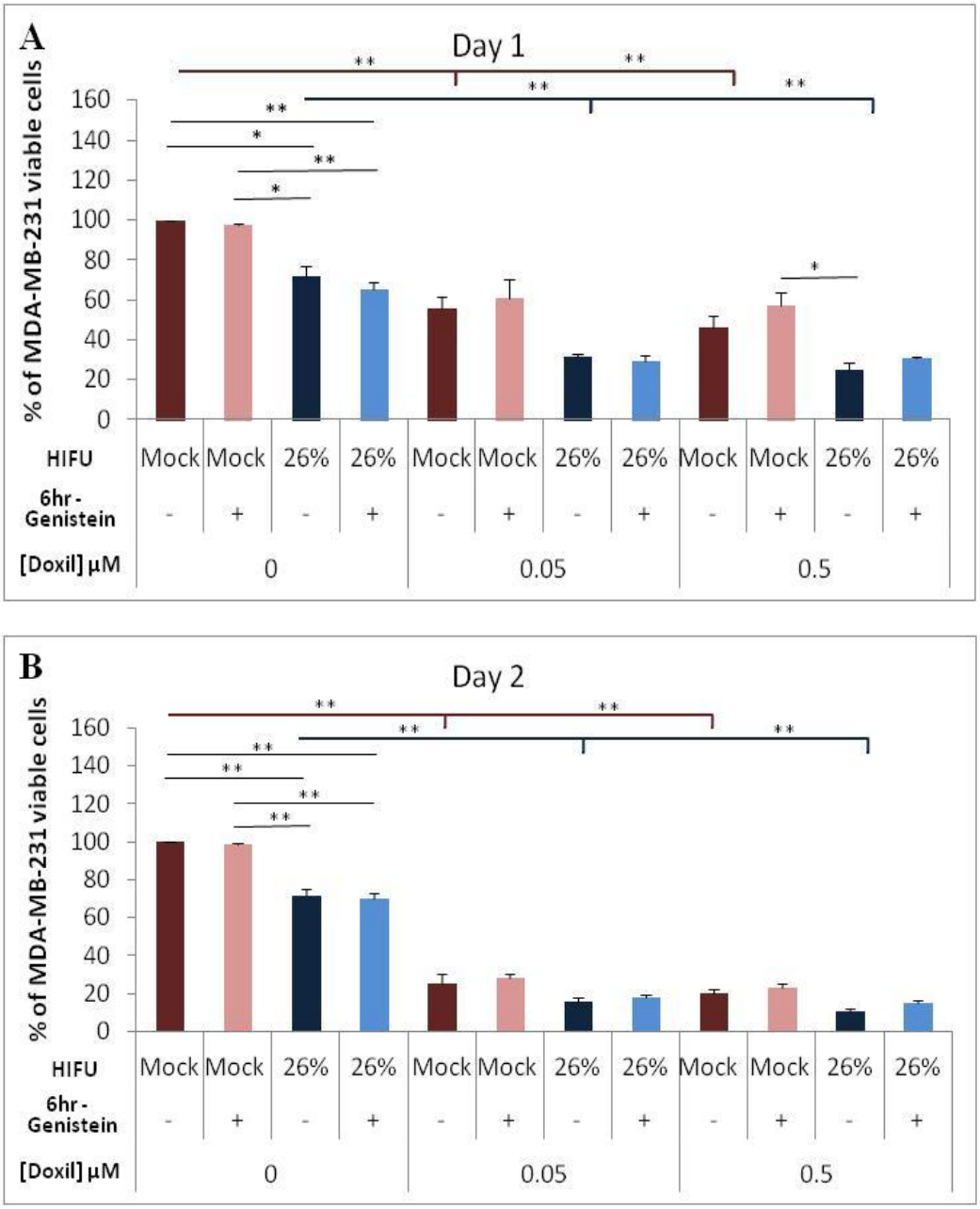

Figure 17: MDA-MB-231 cell viability following Doxil and Genistein pretreatment at 6hr post sub-lethal HIFU exposure (26%). Trypan blue vital stain exclusion assay was used to count viable cells over a period of four days. Trypan blue assessment suggests that there is an enhanced *in vitro* sensitivity of MDA-MB-231 cells to sub-cytotoxic doses of Doxil post sub-lethal HIFU and this sensitivity is reversed in part by the addition of Genistein, yet it was not determined to be statistically significant. Data represent mean percentage ± SEM of 3 independent experiments (each done in duplicates; ** $p<0.05$; **$p<0.01$*).

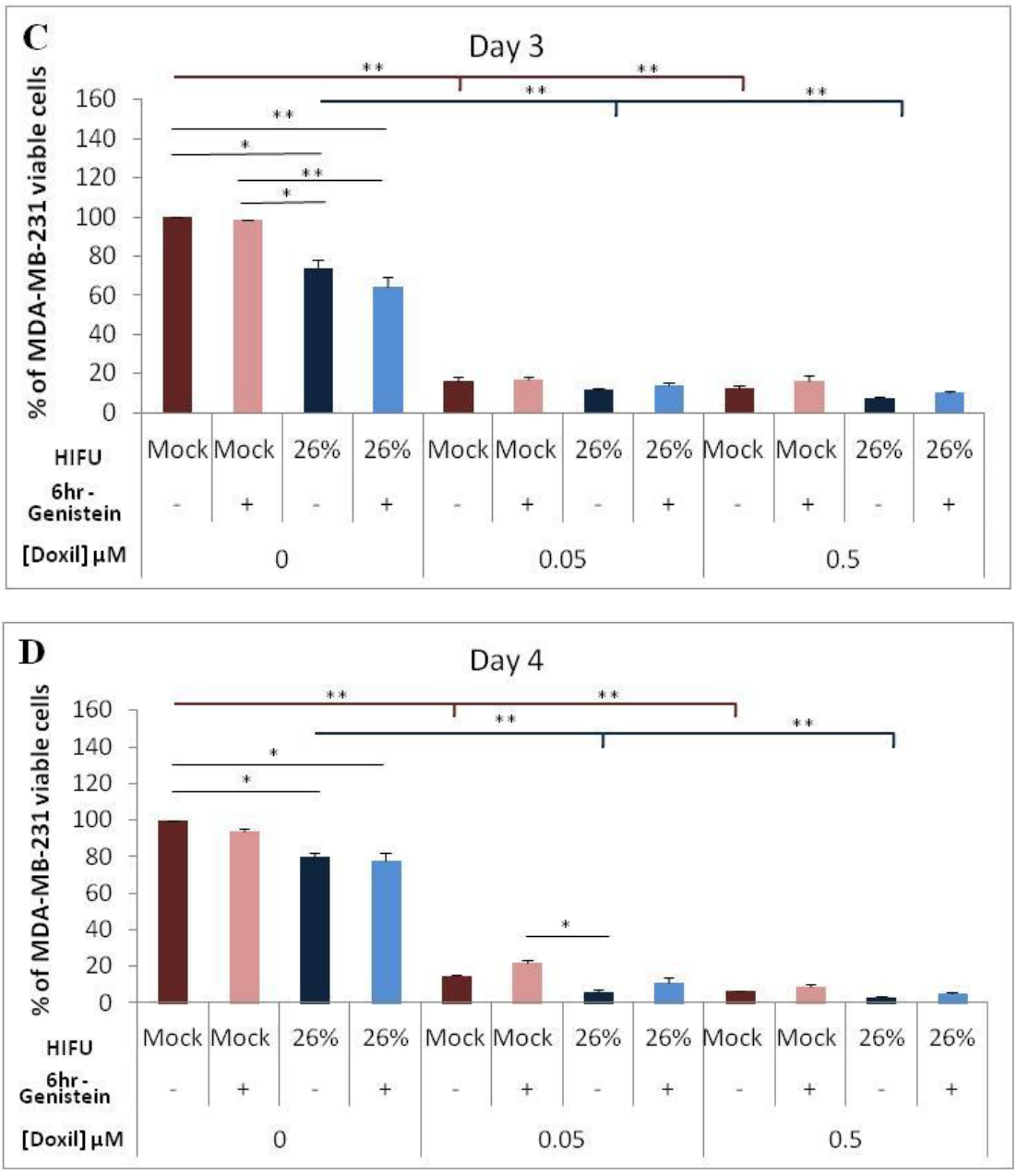

Figure 17: MDA-MB-231 cell viability following Doxil and Genistein pretreatment at 6hr post sub-lethal HIFU exposure (26%). Trypan blue vital stain exclusion assay was used to count viable cells over a period of four days. Trypan blue assessment suggests that there is an enhanced *in vitro* sensitivity of MDA-MB-231 cells to sub-cytotoxic doses of Doxil post sub-lethal HIFU and this sensitivity is reversed in part by the addition of Genistein, yet it was not determined to be statistically significant. Data represent mean percentage ± SEM of 3 independent experiments (each done in duplicates; ** $p<0.05$; **$p<0.01$*).

4. Quantitative assessment of Genistein and Doxil added to MDA-MB- 231 cells 30 hours post sub-lethal HIFU exposure.

Similarly to the assessment of Genistein and Doxil added to MDA-MB-231 cells 6 hours post sub-lethal HIFU exposure, we wanted to assess it 30 hours post sub-lethal HIFU exposure. At Day 1, for cells treated with 0 µM of doxorubicin, trypan blue assessment showed no significant difference in cellular viability between any of the tested samples with a (*P-value>0.05*). As for cells treated with 0.05 µM of doxorubicin, a 20% decrease in cellular viability was obtained in cells exposed to sub-lethal HIFU and untreated with Genistein when compared to mock HIFU cells untreated with Genistein. This decrease was shown to be statistically significant with a (*P-value<0.01*). Moreover, cellular viability was decreased by 14% in cells exposed to sub-lethal HIFU and treated with Genistein and by 25% in cells exposed to sub-lethal HIFU and untreated with Genistein in comparison to mock HIFU cells untreated with Genistein. The latter reduction was shown to statistically significant with a (*P-value<0.05*) while the former reduction was shown to be statistically significant with a (*P-value<0.01*). Noteworthy, cellular viability was enhanced by 11% in cells exposed to sub-lethal HIFU and treated with Genistein in comparison to cells exposed to sub-lethal HIFU and untreated with Genistein. However, this increase, was shown not to be statistically significant (*P-value>0.05*). Likewise for cells treated with 0.5 µM of doxorubicin, cellular viability was increased by 16% in mock control cells treated with Genistein and by 8% in sub-lethal HIFU exposed cells treated with Genistein in comparison to mock control cells untreated with Genistein and sub-lethal HIFU cells untreated with Genistein respectively. This reversal in cellular viability was not shown to be statistically

significant (*P-value>0.05*). Moreover, a significant decrease by 29% with a (*P-value<0.05*) was observed in sub-lethal HIFU cells treated with Genistein relative to mock control cells treated with Genistein. Data represent mean percentage difference ± SEM of three independent experiments, each done in duplicates (Figure 18A, see below).

At day 2, for cells treated with 0 µM, 0.05 µM, and 0.5 µM of doxorubicin, trypan blue assessment revealed a similar pattern to the cells treated with 0 µM doxorubicin, 0.05 µM of doxorubicin, and 0.5 µM of doxorubicin at day 2 post 6hr of sub-lethal HIFU exposure. Data represent mean percentage difference ± SEM of three independent experiments, each done in duplicates. (Figure 18B, see below).

At day 3, for cells treated with 0 µM doxorubicin, trypan blue assessment revealed a similar pattern to that obtained in cells treated with 0 nM of Taxol at day1, 30 hours post sub-lethal HIFU exposure. As for cells treated with 0.05 µM doxorubicin, cellular viability was increased by 11% in mock HIFU cells treated with Genistein when compared to mock HIFU cells untreated with Genistein and by 17% in sub-lethal HIFU exposed cells treated with Genistein when compared to sub-lethal HIFU exposed cells untreated with Genistein. This reversal in cellular viability was not shown to be statistically significant (*P-value>0.05*). A 21% decrease in cellular viability was shown to be statistically significant with a (*P-value<0.05*) in sub-lethal HIFU exposed cells in comparison to mock control cells treated with Genistein. As for cells treated with 0.5 µM of doxorubicin, 18% increase in cellular viability was obtained in mock HIFU cells treated with Genistein and sub-lethal HIFU exposed cells treated with Genistein in comparison to mock HIFU cells untreated with Genistein and sub-lethal HIFU cells untreated with Genistein. This was shown to be

statistically significant with a (*P-value<0.05*). Moreover, a 28% significant decrease in cellular viability with a (*P-value<0.01*) was determined in sub-lethal HIFU exposed cells in comparison to mock HIFU cells treated with genistein. Data represent mean percentage difference ± SEM of three independent experiments, each done in duplicates (Figure 18C, see below).

At day 4, for cells treated with 0 µM doxorubicin, trypan blue assessment revealed a similar pattern to that obtained in cells treated with 0 nM of Taxol at day1, 30 hours post sub-lethal HIFU exposure. As for cells treated with 0.05 µM doxorubicin, a similar pattern was obtained to the cells treated with the same concentration of doxorubicin at day 3. Moreover, cellular viability was increased by 16% in mock HIFU cells treated with Genistein and by 20% in sub-lethal HIFU exposed cells treated with Genistein in comparison to mock HIFU cells untreated with Genistein and sub-lethal HIF U cells untreated with Genistein respectively. This reversal in cellular viability was shown to be statistically significant with a (*P-value<0.05*) for the latter and with a (*P-value<0.01*) for the former. As for cells treated with 0.5 µM doxorubicin, cellular viability was increased by 18% in mock HIFU cells treated with Genistein in comparison to mock HIFU cells untreated with genistein with a (*P-value<0.05*). Data represent mean percentage difference ± SEM of three independent experiments, each done in duplicates (Figure 18D, see below).

Across all days, percentage of cellular viability of mock HIFU cells treated with 0.5µM of doxorubicin and mock HIFU cells treated with 0.05 µM of doxorubicin were significantly reduced in comparison to mock HIFU cells treated with 0 µM of doxorubicin (*P-value<0.01*). Likewise, percentage of cellular viability of sub-lethal HIFU cells treated

with 0.5µM of doxorubicin and mock HIFU cells treated with 0.05 µM of doxorubicin were significantly reduced in comparison to mock HIFU cells treated with 0 µM of doxorubicin (*P-value<0.01*).

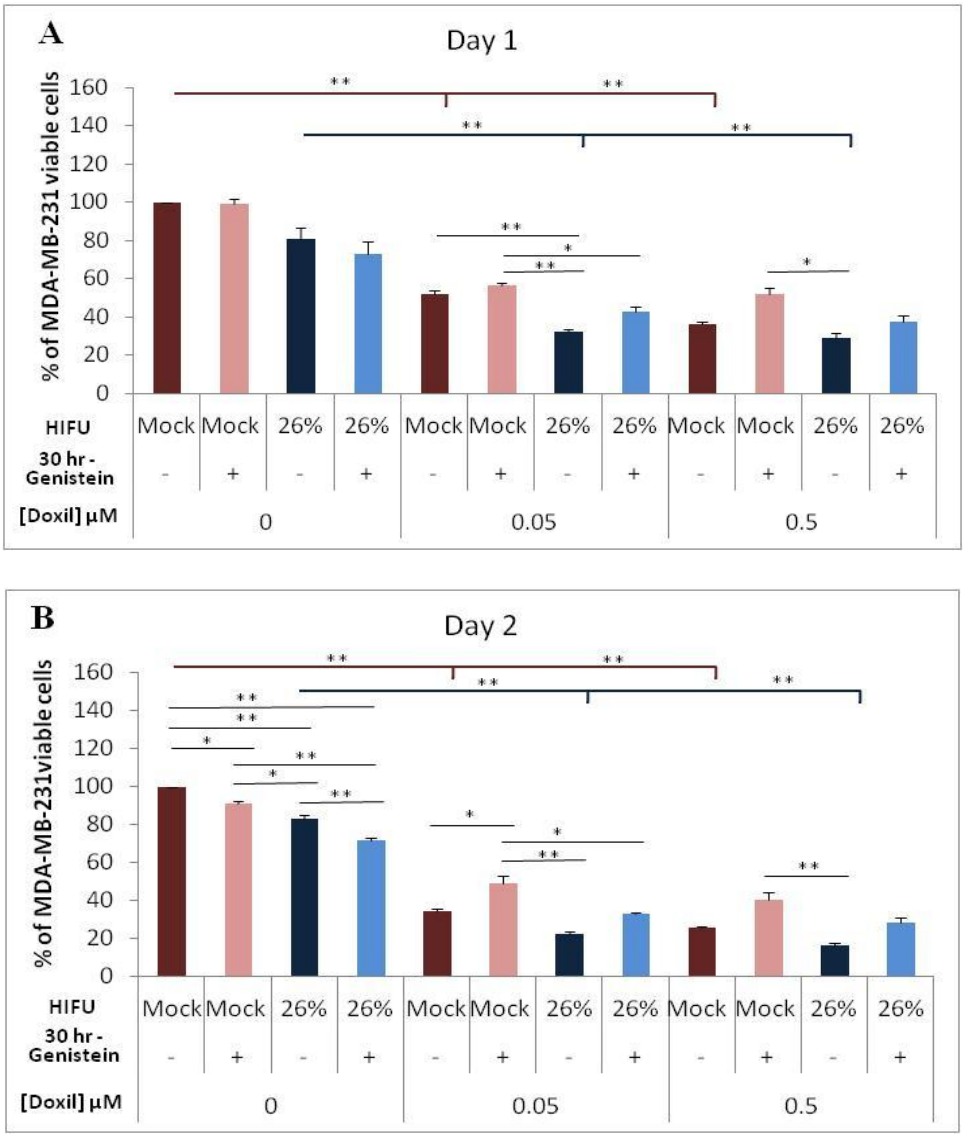

Figure 18: MDA-MB-231 cell viability following Doxil and Genistein pretreatment at 30hr post sub-lethal HIFU exposure (26%). Trypan blue vital stain exclusion assay was used to count viable cells over a period of four days. Trypan blue assessment suggests that there is an enhanced *in vitro* sensitivity of MDA-MB-231 cells to sub-cytotoxic doses of Doxil post sub-lethal HIFU and this sensitivity is reversed by the addition of Genistein, and was determined to be statistically significant at day 3 and day 4. Data represent mean percentage ± SEM of 3 independent experiments (each done in duplicates; ** p<0.05; **p<0.01*).

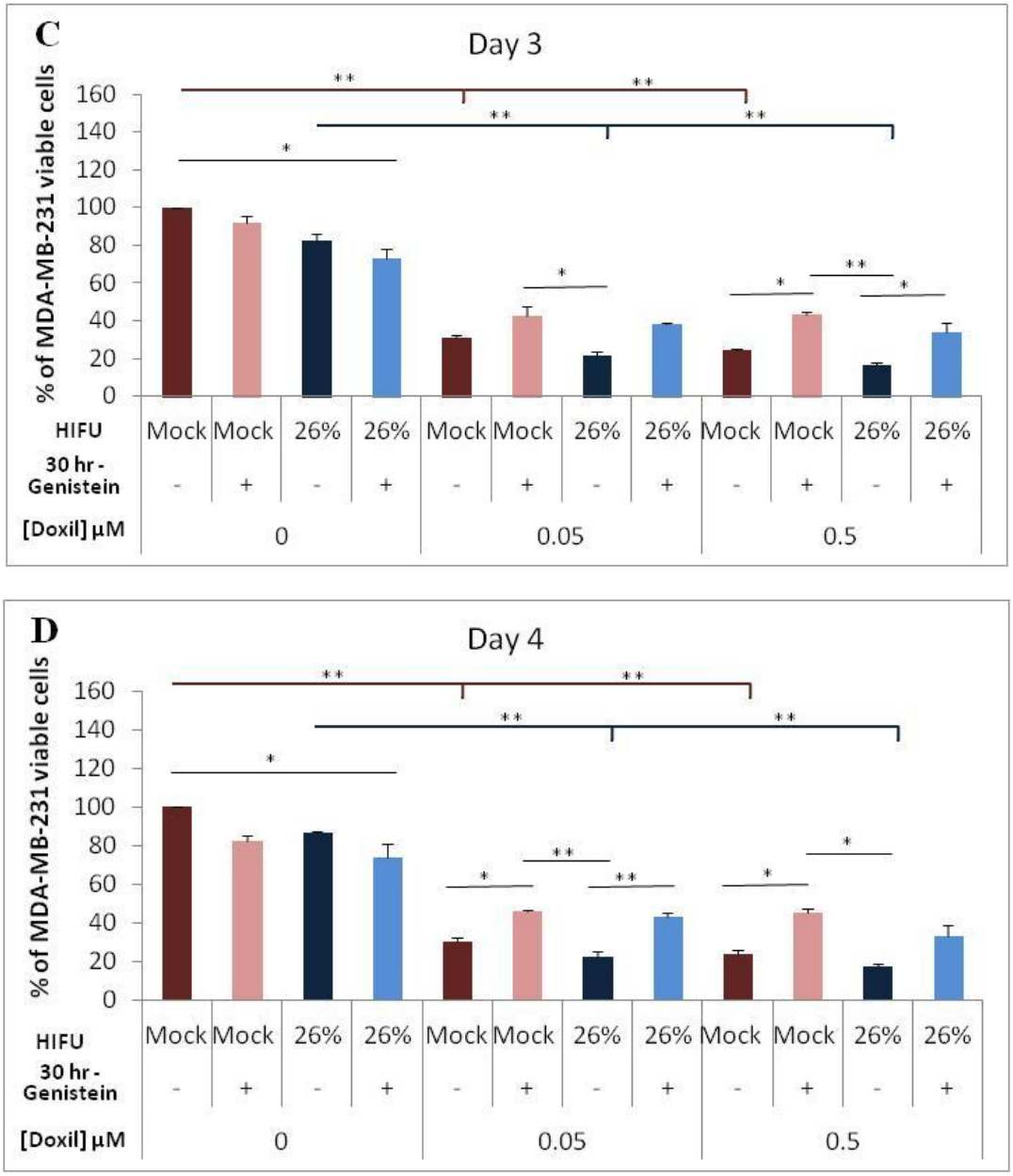

Figure 18: MDA-MB-231 cell viability following Doxil and Genistein pretreatment at 30hr post sub-lethal HIFU exposure (26%). Trypan blue vital stain exclusion assay was used to count viable cells over a period of four days. Trypan blue assessment suggests that there is an enhanced *in vitro* sensitivity of MDA-MB-231 cells to sub-cytotoxic doses of Doxil post sub-lethal HIFU and this sensitivity is reversed by the addition of Genistein, and was determined to be statistically significant at day 3 and day 4. Data represent mean percentage ± SEM of 3 independent experiments (each done in duplicates; * $p<0.05$; ** $p<0.01$).

CHAPTER IV

DISCUSSION

Surgical treatment in combination with other types of systemic treatment has always been considered to be the first line of attack against most breast cancer cases. However, in recent years, aside from the standard treatment methods, there has been much attention in non-invasive treatment modalities for breast cancer, including HIFU. The use of HIFU has been growing rapidly in the biomedical field particularly with the guidance of magnetic resonance imaging. Nevertheless, the effects of sub-lethal HIFU exposure on cell function are not well understood. Previous work from our laboratory showed that sub-lethal HIFU exposure of MDA-MB-231 breast cancer cells *in vitro* results in significant alterations in transcript expression of a number of mechanosensitive genes, including *Cav-1* gene (α-isoform) which encodes for caveolin-1 protein. Moreover, there was enhanced cellular sensitivity to suboptimal cytotoxic doses of Paclitaxel and Doxorubicin. In this study, we aim to identify the mechanisms implicated in the enhanced *in vitro* sensitivity of MDA-MB-231 cells to anti-neoplastic agents post sub-lethal HIFU exposure. Hence, we utilized a commercial HIFU transducer (frequency of 0.500 MHz) that is obtained by the laboratory of Dr. Ghanem Oweis from Sonic Concepts; the manufacturer and developer of a variety of products which include standard and custom HIFU transducers, Washington, USA. The HIFU setup pertaining to cell suspension and exposure was co-designed and manufactured by Dr.Ghanem Oweis's Laboratory, at the Department of Mechanical Engineering, FEA, AUB, in Beirut, Lebanon. It closely mimics the HIFU models that have

been reported in several *in vitro* testing studies (Liu et al., 2005). Because we are utilizing a different HIFU transducer than the one previously used in our laboratory, and because its circumference is much larger, we had to perform numerous optimization trials to ensure reproducibility of the experimental parameters. As a result, we were unable to use all the parameters previously used by my colleagues (Younes, MSc; Malkhasian, MSc). From the sub-lethal HIFU exposures previously used in our laboratory; 75% and 83%, resulted in nearly complete cell death since they fell within the large focal point range. Hence, we had to discard them and pick a parameter that is sub-lethal and also reproducible. Thus, we chose 25.7% HIFU exposure since it was consistent and reproducible across independent experiments. We performed several experimental trials to quantitatively assess cell viability of MDA-MB-231 cells post sub-lethal HIFU exposure in comparison to cells exposed to focal point and mock HIFU cells. Trypan blue assessment method revealed a significant change between the mock HIFU cells and cells exposed to focal point. It is worth mentioning that cells subjected to sub-lethal HIFU were significantly different from the mock control cells at day 2 and day 3 which means their cell viability is compromised in comparison to mock control cells. On the other hand, this obvious decrease in cell viability was revealed between sub-lethal HIFU cells and mock HIFU cells but was not determined to be statistically significant by (Younes, MSc; Malkhasian, MSc). Nevertheless, a significant difference was observed between sub-lethal HIFU cells and cells exposed to focal point which means that despite that sub-lethal HIFU cells are compromised in terms of their cell viability in comparison to mock HIFU cells, they are still by far different from the cells exposed to focal point and still considered by far a sub-lethal exposure. Noteworthy, we tried to utilize HIFU exposures lower than that of 25.7% but we still faced issues with reproducibility.

Our objective was to decipher the possible mechanisms implicated in the enhanced *in vitro* sensitivity to anti-neoplastic agents either 6hr or 30 hr post sub-lethal HIFU exposure. These 2 time points were selected to reflect on the results previously obtained in our laboratory which were initially chosen because they reveal the early and delayed protein expression onset correspondingly. Our first aim under our objective was to determine if sonoporation plays a role in the enhanced *in vitro* sensitivity to anti-neoplastic agents post sub-lethal HIFU exposure. For that, we assessed the uptake of FITC-dextran, a marker for cell permeability, in mock-treated controls versus sub-lethal HIFU-treated MDA-MB-231 cells. Based on manufactured type, dextran varies in size. Dextran, of size 70kDa, used in this study can penetrate into the cytosol if cell membrane is made permeable to it (Meijering et al., 2009). Flow cytometry data analysis suggests that there is a slight increase in the uptake of FITC-dextran in sub-lethal HIFU treated cells in comparison to mock HIFU treated cells but the difference between them is not significant. It is worth mentioning here that under normal circumstances, FITC-dextran should not be able to cross the membrane (Forbes et al., 2011). However, the fact that we could see positive cells for FITC-dextran in mock HIFU treated cells could be in part due to that these cells are stressed since they have been placed in suspension for around 30 minutes while taken to the engineering department. Their cell membrane structure might have been affected in a certain way because they are no longer adhered to their substratum (Ruddon, 2003). It is plausible that stress induced plasma membrane injury on the cells due to the mechanical activity imposed on them. The impact of stress on cancer cell membrane is poorly understood, yet, cancer cells depend on an effective plasma membrane repair that uses different machinery to help repair the damaged plasma membrane (Nylandsted, 2015). Hence, this might suggest a transient pore formation

on the cell membrane that might have resulted in the uptake of some FITC-dextran without compromising the viability of the cells. Moreover, a second factor that may explain this is that the percentage of positive cells detected in mock treated controls probably pertains to the FITC-dextran bound to the cell membrane since FITC-dextran can attach to the exterior of the cell if remaining on the monolayer for a long period of time (Forbes et al., 2011) and this might be the case since flow cytometry detects membrane bound signals as well as to cytoplasmic signals. Despite that we have performed several washing steps, it might not have been sufficient to remove the fluorescent dextran stuck to the surface of the cell. This was a concern as we didn't know to what extent the external binding of FITC-dextran to the cell membrane masked the internalized FITC-dextran. Hence, it would be essential to minimize the fluorescence obtained due to this attached FITC-dextran on the cell membrane. To do so, one of our future aims could be to perform trypan blue quenching, a technique that can minimize the fluorescence of fluorescent molecules attached to the surface of cells, but not internalized (Haugland, 2005). Nevertheless, under the parameters we have studied, flow cytometry might not have been the optimal method to detect uptake of FITC-dextran. Besides, we attempted to assess the uptake of FITC-dextran 6 hours post HIFU exposure (data not shown); however, we faced technical difficulties as we couldn't acquire a sufficient event rate to assess and analyze the results. This emphasized the need for us to assess the uptake of FITC-dextran post sub-lethal HIFU exposure by another method; laser confocal microscopy.

The uptake of FITC-dextran in mock HIFU cells vs. sub-lethal HIFU treated cells 30 hours post sub-lethal HIFU exposure was further validated by laser confocal microscopy. Representative images and visual scoring have shown similar results to

quantification data obtained by flow cytometry. However, the percentage of positive cells scored in mock treated HIFU cells is much lower than that obtained by flow cytometry. This is because while scoring for positive cells visually, we were able to distinguish between cytoplasmic signal and membrane bound signal. Nevertheless, laser confocal microscopy images and visual scoring analysis reveals that there is no significant change in the uptake of FITC-dextran in mock treated HIFU cells vs. sub-lethal HIFU cells 30 hours post HIFU exposure. Moreover, unlike from that obtained by flow cytometry, a significant difference was obtained between the positive control used and mock HIFU treated controls or sub-lethal HIFU cells in the scoring analysis. This further supports our assumption that by laser confocal microscopy we were able to distinguish between the internalized signal and membrane bound signal reducing the effect of the external binding of FITC-dextran on the results. Likewise, similar results were obtained 6 hours post sub-lethal HIFU exposure by laser confocal microscopy indicating no significant change in the uptake of FITC-dextran. This indicates that sonoporation is not implicated, significantly, in the uptake of FITC-dextran in sub-lethal HIFU cells at the experimental parameters we have tested and as assessed by flow cytometry and laser confocal microscopy. Nonetheless, it would be interesting and essential to assess whether sonoporation plays a role at other sub-lethal HIFU parameters. In addition, sonoporation has been reported to impact the structure of organelles (Zeghimi et al., 2012). Therefore, it is plausible that sub-lethal HIFU exposure alters the structure and/or number of membrane caveolae in cells. Our future aims could employ the use of scanning electron microscopy (SEM) to identify any structural changes mainly in the shape, and number of membrane caveolae between sub-lethal HIFU cells and mock HIFU cells.

As for the second aim of the study, we first had to optimize the concentration of Genistein used to inhibit caveolae-dependent endocytosis. Noteworthy, Genistein is not only a tyrosine kinase inhibitor which causes disturbance of the actin filament network at the site of endocytosis and inhibits the sequestering of dynamin II, but has also been reported to have anti-cancer properties by inducing cytotoxicity at specified concentrations in breast cancer cell lines such as MCF-7 (Avci et al., 2015) and inhibiting proliferation as well as inducing cell apoptosis in MDA-MB-231 cells via the mitogen-activated protein kinase pathway (Li et al., 2008). From existing literature, different concentrations of Genistein were used to inhibit caveolae-dependent endocytosis. Hence, we had to try various concentrations and incubation times to find a concentration that not only inhibits caveolae-dependent endocytosis but also does not compromise cell viability. As a result, we used 100 µM of Genistein which has also been used in other studies to inhibit entry of viruses including irodovirus by caveolae-dependent endocytosis (Guo et al., 2011).

The rationale behind our interest in assessing whether caveolae-dependent endocytosis might play a role in the enhanced *in vitro* sensitivity to anti-neoplastic agents post sub-lethal HIFU exposure stems from the fact that previous work from our laboratory showed that sub-lethal HIFU exposure of MDA-MB-231 cells *in vitro* results in an increased expression of the mechanosensitive gene, *Cav-1* gene (α-isoform), which encodes for caveolin-1 protein and since we know that caveolae formation is defined mainly by the expression of caveolin-1 protein, we hypothesized that caveolae-dependent endocytosis is implicated. Similarly to previous results obtained in our laboratory, trypan blue assessment of cell viability has shown that generally across both time points and

across all days Taxol has a more effective killing effect than doxorubicin has on MDA-MB-231 cells. Additionally, enhanced *in vitro* sensitivity of MDA-MB-231 cells was obtained to Taxol at all days whether 6 or 30 hours post HIFU exposure. Noteworthy, since our trypan blue assessment of cell viability at the beginning of the study revealed a significant difference between mock HIFU cells and sub-lethal HIFU cells, we observed a similar result for the assessment of cell viability following Taxol treatment. Nevertheless, this significant difference retained with the addition of the different concentrations of Taxol. Additionally, it is worth mentioning that both mock HIFU cells and sub-lethal HIFU cells treated with the different concentrations of Taxol were significantly different in comparison to their control cells untreated with Taxol. This is indicative of a synergistic effect similarly to that obtained by our lab in a previous study. Moreover, cell viability of mock HIFU cells was not compromised when Genistein was added except when it was added to cells treated with 1.5 nM Taxol at day 3 at both the 6 hr and 30 hr time point. This implies that Taxol under standard conditions (without HIFU) relies mainly on mechanisms other than caveolae-dependent endocytosis such as passive diffusion (Önyüksel et al., 2009). Similar results were obtained when Genistein was added to the sub-lethal HIFU cells. No significant effect was determined on the cell viability of sub-lethal cells treated with Genistein in comparison sub-lethal HIFU cells untreated with Genistein. This implies that post HIFU exposure, and following Taxol treatment, caveolae-dependent endocytosis does not seem to play a major role in the sensitivity of cells to Taxol. Yet, it might have been shown to be more apparent have we used a higher concentration of Genistein.

As for the results obtained following Doxil treatment, both mock HIFU cells and sub-lethal HIFU cells treated with the different concentrations of Doxil were significantly different in comparison to their control cells untreated with Doxil. Moreover, it is apparent that the addition of Genistein to mock HIFU cells resulted in an increase in cell viability in cells treated with Genistein in comparison to mock HIFU cells untreated with Genistein and this was mainly observed at the 30 hour time point. Hence, this suggests the implication of caveolae-dependent endocytosis and could be explained by the fact that the doxorubicin used in this study is a liposomal complex (referred to as Doxil) and it is reported that while free drugs enter cells mostly through passive diffusion or active transport, nano-sized formulations of drugs including liposomes, nanoparticles, and polymeric micelles enter cells via endocytosis (Kou et al., 2013; Chen & Li, 2015). Interestingly, a study by Li and colleagues has shown that folate micelles, conventional nanocarriers, can deliver doxorubicin into cells by caveolae-dependent endocytosis among other mechanisms (Li et al., 2014). Moreover, another study has shown that dox nanocomplexes are uptaken by human neuroblastoma *cell* line by several endocytic pathways with caveolae-mediated endocytosis being the leading mechanism (Sevimli et al., 2015). Moreover, an increase in cell viability following Genistein treatment was also observed in sub-lethal HIFU cells treated with Genistein in comparison to sub-lethal HIFU cells untreated with Genistein. This goes in tandem with the previous results obtained from our laboratory that revealed an increase in Cav-1α gene expression 24 hr post HIFU exposure in MDA-MB-231 cells (Younes, MSc). Caveolae-dependent endocytosis, among other endocytic routes, serves as a pathway in the sensitivity observed of the cells to Doxil using the regions of the

cytoplasmic membrane rich in the Cav-1 protein. Macropinocytosis and clathrin-mediated endocytosis might have also been implicated in tandem with caveolae-dependent endocytosis. A study has shown the roles of the three pathways in the cellular uptake of liposomes containing Doxil following ultrasound exposure (Afadzi et al., 2013). Our results indicate that caveolae-dependent endocytosis is implicated mainly in the enhanced *in vitro* sensitivity of MDA-MB-231 cells to Doxil 30 hours post sub-lethal HIFU and minimally to Taxol 6 hours and 30 hours post sub-lethal HIFU exposure. One of our future aims could be to use short interfering RNA (siRNA) to silence Cav-1 gene (α-isoform) and then check if the enhanced sensitivity obtained is indeed related to the expression of the Cav-1 gene (α-isoform gene) and thus implication of caveolae-dependent endocytosis.

Our findings provide an insight into the putative mechanisms implicated in the enhanced *in vitro* sensitivity of MDA-MB-231 breast cancer cells to sub-cytotoxic doses of Taxol and Doxil post sub-lethal HIFU exposure. Moreover, while Genistein has shown in several testing studies to have anti-cancer effects, in this study, Genistein has shown to serve as an antagonist inhibiting caveolae-dependent endocytosis instead of causing cytotoxicity. Advancement in this context might unravel many clues related to the use of Genistein in cancer therapy.

REFERENCES

Afadzi, M., Strand, S. P., Nilssen, E. A., Masoy, S. E., Johansen, T. F., Hansen, R., ... & de L Davies, C. (2013). Mechanisms of the ultrasound-mediated intracellular delivery of liposomes and dextrans. *Ultrasonics, Ferroelectrics, and Frequency Control, IEEE Transactions on*, *60*(1).

American Cancer Society. Breast Cancer Facts & Figures 2015-2016. Atlanta: American Cancer Society, Inc. 2015.

Anderson, R. G. (1998). The caveolae membrane system. *Annual review of biochemistry*, *67*(1), 199-225.

Avci, C. B., Susluer, S. Y., Caglar, H. O., Balci, T., Aygunes, D., Dodurga, Y., & Gunduz, C. (2015). Genistein-induced mir-23b expression inhibits the growth of breast cancer cells. *Contemporary Oncology*, *19*(1), 32.

Badve, S., Dabbs, D. J., Schnitt, S. J., Baehner, F. L., Decker, T., Eusebi, V., Fox, S.B., Ichihara, S., Jacquemier, J., Lakhani, S.R & Palacios, J. (2011). Basal-like and triple-negative breast cancers: a critical review with an emphasis on the implications for pathologists and oncologists. *Modern Pathology*, *24*(2), 157-167.

Barbuti, A. M., & Chen, Z. S. (2015). Paclitaxel Through the Ages of Anticancer Therapy: Exploring Its Role in Chemoresistance and Radiation Therapy. *Cancers*, *7*(4), 2360-2371.

Blum, R. H., & Carter, S. K. (1974). Adriamycin: a new anticancer drug with significant clinical activity. *Annals of internal medicine*, *80*(2), 249-259.

Book, M. O. (2015). FDA Clears Focused Ultrasound System for Prostate Cancer Treatment.

Boolbol, S. K., & Cate, S. P. (2015). Role of ablation in the treatment of breast cancer: A review. *World J Surg Proced*, *5*(1), 106-110.

Buchholz, T. A., & Wazer, D. E. (2002, October). Molecular biology and genetics of breast cancer development: a clinical perspective. In *Seminars in radiation oncology* (Vol. 12, No. 4, pp. 285-295). WB Saunders.

Cavallo Marincola, B., Pediconi, F., Anzidei, M., Miglio, E., Di Mare, L., Telesca, M., ... & Napoli, A. (2015). High-intensity focused ultrasound in breast pathology: non-invasive treatment of benign and malignant lesions. *Expert review of medical devices*, *12*(2), 191-199.

Chabner, B. A., & Roberts, T. G. (2005). Chemotherapy and the war on cancer. *Nature Reviews Cancer*, *5*(1), 65-72.

Chandra, D., Jahangir, A., Cornelis, F., Rombauts, K., Meheus, L., Jorcyk, C. L., & Gravekamp, C. (2016). Cryoablation and Meriva have strong therapeutic effect on triple-negative breast cancer. *OncoImmunology*, *5*(1), e1049802.

Chatterjee, M., Ben-Josef, E., Thomas, D. G., Morgan, M. A., Zalupski, M. M., Khan, G., ... & Bekaii-Saab, T. (2015). Caveolin-1 is associated with tumor progression and confers a multi-modality resistance phenotype in pancreatic cancer. *Scientific reports*, *5*.

Chen, Y., & Li, T. (2015). Cellular uptake mechanism of paclitaxel nanocrystals determined by confocal imaging and kinetic measurement. *The AAPS journal*, *17*(5), 1126-1134.

Ciocca, D. R., Cuello-Carrión, F. D., Natoli, A. L., Restall, C., & Anderson, R. L. (2012). Absence of caveolin-1 alters heat shock protein expression in spontaneous mammary tumors driven by Her-2/neu expression.*Histochemistry and cell biology*, *137*(2), 187-194.

Cowin, P., & Wysolmerski, J. (2010). Molecular mechanisms guiding embryonic mammary gland development. *Cold Spring Harbor perspectives in biology*, *2*(6), a003251.

Cranston, D. (2015). A review of high intensity focused ultrasound in relation to the treatment of renal tumours and other malignancies. *Ultrasonics sonochemistry*, *27*, 654-658.

Dezhenkova, L. G., Tsvetkov, V. B., & Shtil, A. A. (2014). Topoisomerase I and II inhibitors: chemical structure, mechanisms of action and role in cancer chemotherapy. *Russian Chemical Reviews*, *83*(1), 82.

Engelman, J. A., Wykoff, C. C., Yasuhara, S., Song, K. S., Okamoto, T., & Lisanti, M. P. (1997). Recombinant expression of caveolin-1 in oncogenically transformed cells abrogates anchorage-independent growth. *Journal of Biological Chemistry*, *272*(26), 16374-16381.

Finn, R. S., Crown, J. P., Lang, I., Boer, K., Bondarenko, I. M., Kulyk, S. O., ... & Shparyk, Y. (2015). The cyclin-dependent kinase 4/6 inhibitor palbociclib in combination with letrozole versus letrozole alone as first-line treatment of oestrogen receptor-positive, HER2-negative, advanced breast cancer (PALOMA-1/TRIO-18): a randomised phase 2 study. *The Lancet Oncology*, *16*(1), 25-35.

Forbes, M. M., Steinberg, R. L., & O'Brien, W. D. (2011). Frequency-dependent evaluation of the role of definity in producing sonoporation of Chinese hamster ovary cells. *Journal of Ultrasound in Medicine*, *30*(1), 61-69.

Fra, A. M., Williamson, E., Simons, K., & Parton, R. G. (1995). De novo formation of caveolae in lymphocytes by expression of VIP21-caveolin. *Proceedings of the National Academy of Sciences*, *92*(19), 8655-8659.

Fu, D., Calvo, J. A., & Samson, L. D. (2012). Balancing repair and tolerance of DNA damage caused by alkylating agents. *Nature Reviews Cancer*, *12*(2), 104-120.

Furusawa, H., Namba, K., Thomsen, S., Akiyama, F., Bendet, A., Tanaka, C., ... & Nakahara, H. (2006). Magnetic resonance–guided focused ultrasound surgery of breast cancer: reliability and effectiveness. *Journal of the American College of Surgeons*, *203*(1), 54-63.

Garcia, S., Dalès, J. P., Charafe-Jauffret, E., Carpentier-Meunier, S., Andrac-Meyer, L., Jacquemier, J., ... & Charpin, C. (2007). Poor prognosis in breast carcinomas correlates with increased expression of targetable CD146 and c-Met and with proteomic basal-like phenotype. *Human pathology*, *38*(6), 830-841.

Gianfelice, D., Khiat, A., Amara, M., Belblidia, A., & Boulanger, Y. (2003). MR imaging–guided focused us ablation of breast cancer: Histopathologic assessment of effectiveness—initial experience 1. *Radiology*, *227*(3), 849-855.

Gjorevski, N. and Nelson, C.M. 2011. Integrated morphodynamic signaling of the mammary gland.*Nat Rev Mol Cell Biol*. 12: 581-93.

González-Sarrías, A., Tomé-Carneiro, J., Bellesia, A., Tomás-Barberán, F. A., & Espín,

Guo, C. J., Liu, D., Wu, Y. Y., Yang, X. B., Yang, L. S., Mi, S., ... & Chen, W. J. (2011). Entry of tiger frog virus (an Iridovirus) into HepG2 cells via a pH-dependent, atypical, caveola-mediated endocytosis pathway. *Journal of virology*, *85*(13), 6416-6426.

Haugland, R. P. (2005). *The handbook: a guide to fluorescent probes and labeling technologies*. Molecular probes.

Hayer, A., Stoeber, M., Bissig, C., & Helenius, A. (2010). Biogenesis of caveolae: stepwise assembly of large caveolin and cavin complexes. *Traffic*,*11*(3), 361-382.

Hehlgans, S., & Cordes, N. (2011). Caveolin-1: an essential modulator of cancer cell radio-and chemoresistance. *Am J Cancer Res*, *1*(4), 521-30.

Hino M, Doihara H, Kobayashi K, Aoe M, Shimizu N (2003). Caveolin-1 as tumor suppressor gene in breast cancer. Surg Today, 33, 486-90.

Hoang, N. H., Murad, H. Y., Ratnayaka, S. H., Chen, C., & Khismatullin, D. B. (2014). Synergistic ablation of liver tissue and liver cancer cells with high-intensity focused ultrasound and ethanol. *Ultrasound in medicine & biology*,*40*(8), 1869-1881.

Huber, P. E., Jenne, J. W., Rastert, R., Simiantonakis, I., Sinn, H. P., Strittmatter, H. J., ... & Debus, J. (2001). A new noninvasive approach in breast cancer therapy using magnetic resonance imaging-guided focused ultrasound surgery. *Cancer research*, *61*(23), 8441-8447.

Inman, J. L., Robertson, C., Mott, J. D., & Bissell, M. J. (2015). Mammary gland development: cell fate specification, stem cells and the microenvironment. *Development*, *142*(6), 1028-1042.

J. C. (2015). The ellagic acid-derived gut microbiota metabolite, urolithin A, potentiates the anticancer effects of 5-fluorouracil chemotherapy on human colon cancer cells. *Food & function*, *6*(5), 1460-1469.

Juliano, R. L., & Ling, V. (1976). A surface glycoprotein modulating drug permeability in Chinese hamster ovary cell mutants. *Biochimica et Biophysica Acta (BBA)-Biomembranes*, *455*(1), 152-162.

Kaye, S. B. (1998). New antimetabolites in cancer chemotherapy and their clinical impact. *British journal of cancer*, *78*(Suppl 3), 1.

Kiss, A. L. (2012). Caveolae and the regulation of endocytosis. In *Caveolins and Caveolae* (pp. 14-28). Springer US.

Kogo, H., Aiba, T., & Fujimoto, T. (2004). Cell Type-specific Occurrence of Caveolin-1α and -1β in the Lung Caused by Expression of Distinct mRNAs. J. Biol. Chem., 279(24), 25574–25581.

Koleske, A. J., Baltimore, D., & Lisanti, M. P. (1995). Reduction of caveolin and caveolae in oncogenically transformed cells. *Proceedings of the National Academy of Sciences*, *92*(5), 1381-1385.

Kotopoulis, S., Dimcevski, G., Gjertsen, B. T., Gilja, O. H., McCormack, E., & Postema, M. (2014, September). Sonoporation: From the lab to human clinical trials. In *Ultrasonics Symposium (IUS), 2014 IEEE International* (pp. 846-849). IEEE.

Kou, L., Sun, J., Zhai, Y., & He, Z. (2013). The endocytosis and intracellular fate of nanomedicines: Implication for rational design. *Asian Journal of Pharmaceutical Sciences*, *8*(1), 1-10.

Lanigan, F., O'Connor, D., Martin, F., & Gallagher, W. M. (2007). Molecular links between mammary gland development and breast cancer. *Cellular and molecular life sciences: CMLS*, *64*(24), 3159-3184.

Lee, C. Y., Lai, T. Y., Tsai, M. K., Ou-Yang, P., Tsai, C. Y., Wu, S. W., Hsu, L.C. & Chen, J. S. (2016). The influence of a caveolin-1 mutant on the function of P-glycoprotein. *Scientific reports*, *6*.

Lee, S. W., Reimer, C. L., Oh, P., Campbell, D. B., & Schnitzer, J. E. (1998). Tumor cell growth inhibition by caveolin re-expression in human breast cancer cells. *Oncogene*, *16*(11), 1391-1397.

Leslie, T., Ritchie, R., Illing, R., Ter Haar, G., Phillips, R., Middleton, M., ... & Cranston, D. (2014). High-intensity focused ultrasound treatment of liver tumours: post-treatment MRI correlates well with intra-operative estimates of treatment volume. *The British journal of radiology*.

Li, Y. J., Huang, G. L., Sun, X. L., Zhao, X. C., & Li, Z. G. (2016). The combination therapy of high-intensity focused ultrasound with radiotherapy in locally advanced pancreatic carcinoma. *World journal of surgical oncology*, *14*(1), 1.

Li, Y. L., Van Cuong, N., & Hsieh, M. F. (2014). Endocytosis pathways of the folate tethered star-shaped PEG-PCL micelles in cancer cell lines. *Polymers*,*6*(3), 634-650.

Li, Z., Li, J., Mo, B., Hu, C., Liu, H., Qi, H., ... & Xu, J. (2008). Genistein induces cell apoptosis in MDA-MB-231 breast cancer cells via the mitogen-activated protein kinase pathway. *Toxicology in vitro*, *22*(7), 1749-1753.

Liu, Y., Kon, T., Li, C., & Zhong, P. (2005). High intensity focused ultrasound-induced gene activation in sublethally injured tumor cells in vitro. *The Journal of the Acoustical Society of America*, *118*(5), 3328-3336.

Lynn, J. G., Zwemer, R. L., Chick, A. J., & Miller, A. E. (1942). A new method for the generation and use of focused ultrasound in experimental biology. *The Journal of general physiology*, *26*(2), 179.

Maloney, E., & Hwang, J. H. (2015). Emerging HIFU applications in cancer therapy. *International Journal of Hyperthermia*, *31*(3), 302-309.

Meijering, B. D., Juffermans, L. J., van Wamel, A., Henning, R. H., Zuhorn, I. S., Emmer, M., ... & de Jong, N. (2009). Ultrasound and microbubble-targeted delivery of macromolecules is regulated by induction of endocytosis and pore formation. *Circulation research*, *104*(5), 679-687.

Meijering, B. D., Juffermans, L. J., van Wamel, A., Henning, R. H., Zuhorn, I. S., Emmer, M., Versteilen, A.M., Paulus, W.J., van Gilst, W.H., Kooiman, K. & de Jong, N. (2009). Ultrasound and microbubble-targeted delivery of macromolecules is regulated by induction of endocytosis and pore formation. *Circulation research, 104*(5), 679-687.

Melamed, S., Goldenfeld, M., Cotlear, D., Skaat, A., & Moroz, I. (2015). High-intensity focused ultrasound treatment in refractory glaucoma patients: results at 1 year of prospective clinical study. *European journal of ophthalmology*, *25*(6), 483-489.

Merckel, L. G., Knuttel, F. M., Deckers, R., van Dalen, T., Schubert, G., Peters, N. H., ... & van Gorp, J. M. (2016). First clinical experience with a dedicated MRI-guided high-intensity focused ultrasound system for breast cancer ablation. *European radiology*, 1-10.

Montesano, R., Roth, J., Robert, A., & Orci, L. (1982). Non-coated membrane invaginations are involved in binding and internalization of cholera and tetanus toxins. *Nature*, *296*, 651-653.

Nabi, I. R., & Le, P. U. (2003). Caveolae/raft-dependent endocytosis. *The Journal of cell biology*, *161*(4), 673-677.

Nomura, T., & Mimata, H. (2012). Focal therapy in the management of prostate cancer: an emerging approach for localized prostate cancer.*Advances in urology*, *2012*.

Nylandsted, J. (2015). Plasma membrane repair provides a new strategy for targeting metastatic cancer cells. *Cancer Cell & Microenvironment*, *2*(1).

Önyüksel, H., Jeon, E., & Rubinstein, I. (2009). Nanomicellar paclitaxel increases cytotoxicity of multidrug resistant breast cancer cells. *Cancer letters*, *274*(2), 327-330.

Orr, G. A., Verdier-Pinard, P., McDaid, H., & Horwitz, S. B. (2003). Mechanisms of Taxol resistance related to microtubules. *Oncogene*, *22*(47), 7280-7295.

Orsi, F., Arnone, P., Chen, W., & Zhang, L. (2010). High intensity focused ultrasound ablation: a new therapeutic option for solid tumors. *Journal of cancer research and therapeutics*, *6*(4), 414.

Palade, G. E. (1953). Fine structure of blood capillaries. *J Appl phys*, *24*(1), 1424-1436.

Parton, R. G., & del Pozo, M. A. (2013). Caveolae as plasma membrane sensors, protectors and organizers. *Nature reviews Molecular cell biology*,*14*(2), 98-112.

Parton, R. G., Hanzal-Bayer, M., & Hancock, J. F. (2006). Biogenesis of caveolae: a structural model for caveolin-induced domain formation. *Journal of cell science*, *119*(5), 787-796.

Pelkmans, L., Kartenbeck, J., & Helenius, A. (2001). Caveolar endocytosis of simian virus 40 reveals a new two-step vesicular-transport pathway to the ER. *Nature cell biology*, *3*(5), 473-483.

Pelkmans, L., Püntener, D., & Helenius, A. (2002). Local actin polymerization and dynamin recruitment in SV40-induced internalization of caveolae. *Science*, *296*(5567), 535-539.

Pelkmans, L., Purterer, D., & Helenius, A. (2002). SV 40 induced internalization of caveolae involves local actin polymerization and dynamin-recruitment. *Science*, *296*, 535-39.

Pérez-Arnaiz, C., Busto, N., Leal, J. M., & García, B. (2014). New insights into the mechanism of the DNA/doxorubicin interaction. *The Journal of Physical Chemistry B*, *118*(5), 1288-1295.

Perkin, A. G., & Newbury, F. G. (1899). LXXIX.—The colouring matters contained in dyer's broom (Genista tinctoria) and heather (Calluna vulgaris). *Journal of the Chemical Society, Transactions*, *75*, 830-839.

Phenix, C. P., Togtema, M., Pichardo, S., Zehbe, I., & Curiel, L. (2014). High intensity focused ultrasound technology, its scope and applications in therapy and drug delivery. *Journal of Pharmacy & Pharmaceutical Sciences*,*17*(1), 136-153.

Prasanna, H.P., Myers, M.R., Robinson, R.A., Maruvada, S.H., Sliwa, J., and Banerjee, R.K. 2008. Characterization of high intensity focused ultrasound transducers using acoustic streaming. *J. Acoust. Soc. Am* 123(3):1706-1719.

Priyadarshini, K. (2013). Paclitaxel against cancer: a short review. *Medicinal Chemistry*, *2012*.

Raghavan KS, Shajahan-Haq AN (2014) Caveolin-1 and Drug Responsiveness in Breast Cancer. JSM Clin Oncol Res 2(5): 1036.

Rejman, J., Bragonzi, A., & Conese, M. (2005). Role of clathrin-and caveolae-mediated endocytosis in gene transfer mediated by lipo-and polyplexes. *Molecular Therapy*, *12*(3), 468-474.

Richterová, Z., Liebl, D., Horák, M., Palková, Z., Štokrová, J., Hozák, P., ... & Forstová, J. (2001). Caveolae are involved in the trafficking of mouse polyomavirus virions and artificial VP1 pseudocapsids toward cell nuclei. *Journal of virology*, *75*(22), 10880-10891.

Rivankar, S. (2014). An overview of doxorubicin formulations in cancer therapy. *Journal of cancer research and therapeutics*, *10*(4), 853.

Rosen, L. S., Ashurst, H. L., & Chap, L. (2010). Targeting signal transduction pathways in metastatic breast cancer: a comprehensive review.*The oncologist*, *15*(3), 216-235.

Rove, K. O., Sullivan, K. F., & Crawford, E. D. (2010). High-intensity focused ultrasound: ready for primetime. *Urologic Clinics of North America*, *37*(1), 27-35.

Ruddon, R. W. (2003). What Makes a Cancer Cell a Cancer Cell?.

Schnitzer, J. E., Oh, P., Pinney, E., & Allard, J. (1994). Filipin-sensitive caveolae-mediated transport in endothelium: reduced transcytosis, scavenger endocytosis, and capillary permeability of select macromolecules. *The Journal of cell biology*, *127*(5), 1217-1232.

Schwartzberg, B. S., Abdelatif, O. M. A., Lewin, J. M., Bernard, J. M., Brehm, J. L., Bu-Ali, H. M., Cawthorn, S.J., Chen-Seeto, M., Feldman, S.M., Govindarajulu, S. & Jones, L. I. (2016). Abstract P3-13-03: Multicenter clinical trial of percutaneous laser ablation for early stage primary breast cancer. Results of 49 cases with radiographic and pathological correlation. *Cancer Research*, *76*(4 Supplement), P3-13.

Sevimli, S., Sagnella, S., Macmillan, A., Whan, R., Kavallaris, M., Bulmus, V., & Davis, T. P. (2015). The endocytic pathway and therapeutic efficiency of doxorubicin conjugated cholesterol-derived polymers. *Biomaterials science*,*3*(2), 323-335.

Subik, K., Lee, J. F., Baxter, L., Strzepek, T., Costello, D., Crowley, P., Xing, L., Hung, M.C., Bonfiglio, T., Hicks, D.G. & Tang, P. (2010). The expression patterns of ER, PR, HER2, CK5/6, EGFR, Ki-67 and AR by immunohistochemical analysis in breast cancer cell lines.*Breast cancer: basic and clinical research*, *4*, 35.

Swain, S. M., Baselga, J., Kim, S. B., Ro, J., Semiglazov, V., Campone, M., ... & Clark, E. (2015). Pertuzumab, trastuzumab, and docetaxel in HER2-positive metastatic breast cancer. *New England Journal of Medicine*, *372*(8), 724-734.

Tacar, O., Sriamornsak, P., & Dass, C. R. (2013). Doxorubicin: an update on anticancer molecular action, toxicity and novel drug delivery systems. *Journal of Pharmacy and Pharmacology*, *65*(2), 157-170.

Ter Haar, G. (2007). Therapeutic applications of ultrasound. *Progress in biophysics and molecular biology*, *93*(1), 111-129.

Tsao, A. S., & Papadimitrakopoulou, V. (2011). Mitotic Inhibitors. *Journal of Thoracic Oncology*, *6*(11), S1789-S1790.

Uchida, T., Tomonaga, T., Kim, H., Nakano, M., Shoji, S., Nagata, Y., & Terachi, T. (2015). Improved outcomes with advancements in high intensity focused ultrasound devices for the treatment of localized prostate cancer. *The Journal of urology*, *193*(1), 103-110.

Uemura, Y., Sasaki, K., Minami, K., Sato, T., Choi, P. K., & Takeuchi, S. (2015). Observation of cavitation bubbles and acoustic streaming in high intensity ultrasound fields. *Japanese Journal of Applied Physics*, *54*(7S1), 07HB05.

Vo, H. Q., Kim, Y. S., & O'Neill, B. E. (2015). Elimination of multi-drug-resistant breast cancer cells using combination of high-intensity focused ultrasound and low-dose generic chemotherapeutic. *Cancer Research*, *75*(15 Supplement), 711-711.

Wang, S., Yang, C., Zhang, J., Kong, X. R., Zhu, H., Wu, F., & Wang, Z. (2014). First experience of high-intensity focused ultrasound combined with transcatheter arterial embolization as local control for hepatoblastoma.*Hepatology*, *59*(1), 170-177.

Wani, M. C., Taylor, H. L., Wall, M. E., Coggon, P., & McPhail, A. T. (1971). Plant antitumor agents. VI. Isolation and structure of taxol, a novel antileukemic and antitumor agent from Taxus brevifolia. *Journal of the American Chemical Society*, *93*(9), 2325-2327.

Watson, C. J., & Khaled, W. T. (2008). Mammary development in the embryo and adult: a journey of morphogenesis and commitment.*Development*, *135*(6), 995-1003.

Weigelt, B., Geyer, F. C., Natrajan, R., Lopez-Garcia, M. A., Ahmad, A. S., Savage, K., ... & Reis-Filho, J. S. (2010). The molecular underpinning of lobular histological growth pattern: a genome-wide transcriptomic analysis of invasive lobular carcinomas and grade-and molecular subtype-matched invasive ductal carcinomas of no special type. *The Journal of pathology*,*220*(1), 45-57.

Wiechen, K., Diatchenko, L., Agoulnik, A., Scharff, K. M., Schober, H., Arlt, K., ... & Sers, C. (2001). Caveolin-1 is down-regulated in human ovarian carcinoma and acts as a candidate tumor suppressor gene. *The American journal of pathology*, *159*(5), 1635-1643.

Wu, F. (2014). High intensity focused ultrasound: a noninvasive therapy for locally advanced pancreatic cancer. *World J Gastroenterol*, *20*(44), 16480-16488.

Wu, P., Qi, B., Zhu, H., Zheng, Y., Li, F., & Chen, J. (2007). Suppression of staurosporine-mediated apoptosis in Hs578T breast cells through inhibition of neutral-sphingomyelinase by caveolin-1. *Cancer letters*, *256*(1), 64-72.

Yamada, E. (1955). The fine structure of the gall bladder epithelium of the mouse. *The Journal of biophysical and biochemical cytology*, *1*(5), 445.

Yokochi, T., & Robertson, K. D. (2004). Doxorubicin inhibits DNMT1, resulting in conditional apoptosis. *Molecular pharmacology*, *66*(6), 1415-1420.

Youlden, D. R., Cramb, S. M., Yip, C. H., & Baade, P. D. (2014). Incidence and mortality of female breast cancer in the Asia-Pacific region. *Cancer biology & medicine*, *11*(2), 101-115.

Zeghimi, A., Uzbekov, R., Arbeille, B., Escoffre, J. M., & Bouakaz, A. (2012, October). Ultrastructural modifications of cell membranes and organelles induced by sonoporation. In *Ultrasonics Symposium (IUS), 2012 IEEE International* (pp. 2045-2048). IEEE.

Zeghimi, A., Uzbekov, R., Arbeille, B., Escoffre, J. M., & Bouakaz, A. (2012, October). Ultrastructural modifications of cell membranes and organelles induced by sonoporation. In *Ultrasonics Symposium (IUS), 2012 IEEE International* (pp. 2045-2048). IEEE.

Zhao, Z., Han, F. H., Yang, S. B., Hua, L. X., Wu, J. H., & Zhan, W. H. (2015). Loss of stromal caveolin-1 expression in colorectal cancer predicts poor survival. *World journal of gastroenterology: WJG*, *21*(4), 1140.

Zhou, Y. (2014). High-intensity focused ultrasound treatment for advanced pancreatic cancer. *Gastroenterology research and practice*, *2014*

Zhou, Y., Yang, K., Cui, J., Ye, J. Y., & Deng, C. X. (2012). Controlled permeation of cell membrane by single bubble acoustic cavitation. *Journal of controlled release*, *157*(1), 103-111.

Shajahan, A. N., Dobbin, Z. C., Hickman, F. E., Dakshanamurthy, S., & Clarke, R. (2012). Tyrosine-phosphorylated caveolin-1 (Tyr-14) increases sensitivity to paclitaxel by inhibiting BCL2 and BCLxL proteins via c-Jun N-terminal kinase (JNK). *Journal of Biological Chemistry*, *287*(21), 17682-17692.